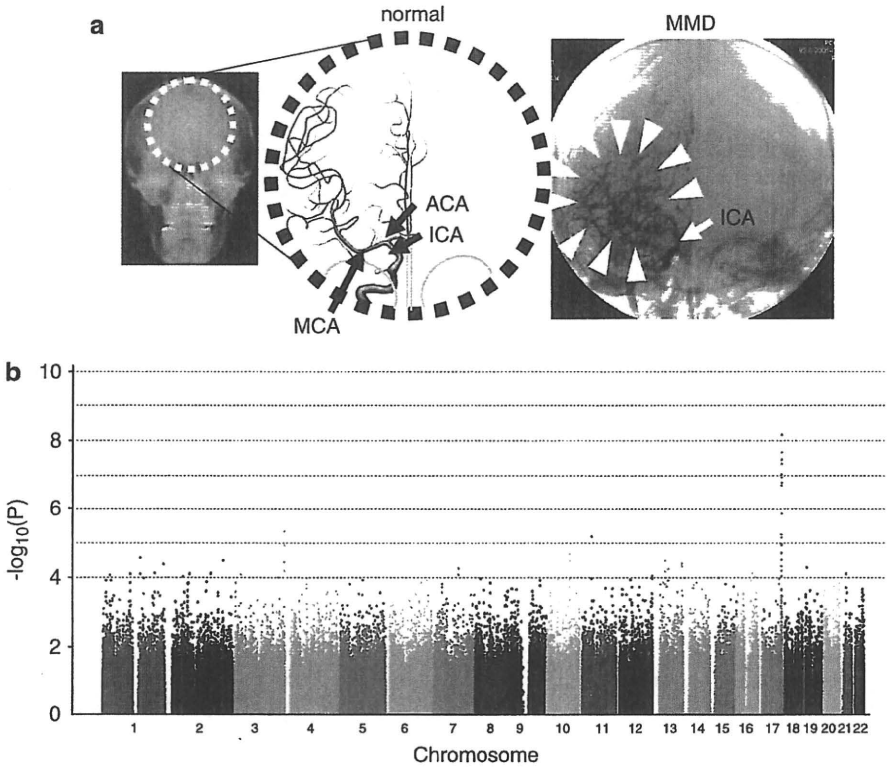

Figure 1 (**a**) Abnormal brain vessels in MMD. The dotted circle indicates the X-ray field of cerebral angiography (left panel). Normal structures of the right internal carotid artery (ICA), anterior cerebral artery (ACA) and middle cerebral artery (MCA) are illustrated (middle panel). The arrowheads indicate abnormal collateral vessels appearing like a puff of smoke in the angiogram of an individual with MMD (right panel). Note that ACA and MCA are barely visible, because of the occlusion of the terminal portion of the ICA. (**b**) Manhattan plot of the 785 720 SNPs used in the genome-wide association analysis of MMD patients. Note that the SNPs in the 17q25-ter region reach a significance of $P<10^{-8}$.

MATERIALS AND METHODS

Affected individuals

Genomic DNA was extracted from blood and/or saliva samples obtained from members of the families with MMD (Supplementary Figure 1), MMD patients with no family history and control subjects. All of the subjects were Japanese. MMD was diagnosed on the basis of guidelines established by the Research Committee on Spontaneous Occlusion of the Circle of Willis of the Ministry of Health and Welfare of Japan. This study was approved by the Ethics Committee of Tohoku University School of Medicine. Total RNA samples were purified from leukocytes using an RNeasy mini kit (Qiagen, Hilden, Germany) and used as templates for cDNA synthesis with an Oligo $(dT)_{20}$ primer and SuperScript II reverse transcriptase according to the manufacturer's instructions (Invitrogen, Carlsbad, CA, USA).

Linkage analysis

For the linkage analysis, DNA samples were genotyped for 36 microsatellite markers within five previously reported MMD loci using the ABI 373A DNA Sequencer (Applied Biosystems, Foster City, CA, USA). Pedigrees and haplotypes were constructed with the Cyrillic version 2.1 software (Oxfordshire, UK). Multipoint analyses were conducted using the GENEHUNTER 2 software (http://www.broadinstitute.org/ftp/distribution/software/genehunter/). Statistical analysis was performed with SPSS version 14.0J (SPSS, Tokyo, Japan).

Genome-wide and locus-specific association studies

A genome-wide association study was performed using a group of 72 MMD patients, which consisted of 64 patients without a family history of MMD and 8 probands of MMD families. The Illumina Human Omni-Quad 1 chip (Illumina, San Diego, CA, USA) was used for genotyping, and single-nucleotide polymorphisms (SNPs) with a genotyping completion rate of 100% were used for further statistical analysis (785 720 out of 1 140 419 SNPs). Genotyping data from 45 healthy Japanese controls were obtained from the database at the International HapMap Project web site. The 785 720 SNPs were statistically analyzed using the PLINK software (http://pngu.mgh.harvard.edu/~purcell/plink/index.shtml). For a locus-specific association study, we used 63 DNA samples consisting of 58 non-familial MMD patients and 5 probands of MMD families. A total of 384 SNPs within chromosome 17q25-ter were genotyped (Supplementary Table 1), using the GoldenGate Assay and a custom SNP chip (Illumina). Genotyping data for 45 healthy Japanese were used as a control. Case–control single-marker analysis, haplotype frequency estimation and significance testing of differences in haplotype frequency were performed using the Haploview version 3.32 program (http://www.broad.mit.edu/mpg/haploview/).

Mutation detection

Mutational analyses of *RNF213* and *FLJ35220* were performed by PCR amplification of each coding exon and putative promoter regions, followed by direct sequencing. Genomic sequence data for the two genes were obtained from the National Center for Biotechnology Information web site (http://www.ncbi.nlm.nih.gov/) for design of exon-specific PCR primers. *RNF213* cDNA fragments were amplified from leukocyte mRNA for sequencing analysis. Sequencing of the PCR products was performed with the ABI BigDye Terminator Cycle Sequencing Reaction Kit using the ABI 310 Genetic Analyzer. Identified base changes were screened in control subjects. Statistical difference of the carrier frequency of each base change was estimated by Fisher's exact test (the MMD group vs the control group).

Quantitative PCR

MTC Multiple Tissue cDNA Panels (Clontech Laboratory, Madison, WI, USA) were the source of cDNAs from human cell lines, adult and fetal tissues. Mononuclear cells and polymorphonuclear cells were isolated from the fresh peripheral blood of healthy human adults using Polymorphprep (Cosmo Bio,

Carlsbad, CA, USA). T and B cells were isolated from the fresh peripheral blood of healthy human adults using the autoMACS separator (Militeny Biotec, Bergisch Gladbach, Germany). Total RNA was isolated from these cells with the RNeasy Mini Kit (Qiagen) following the manufacturer's instructions. We reverse transcribed 100 ng samples of total RNA into cDNAs using the High Capacity cDNA Reverse Transcription Kit (Applied Biosystems). Quantitative PCRs were performed in a final volume of 20 µl using the FastStart TaqMan Probe Master (Rox) (Roche, Madison, WI, USA), 5 µl of cDNA, 10 µM of *RNF*- or *GAPDH*-specific primers and 10 µM of probes (Universal ProbeLibrary Probe #80 for *RNF213* and Roche Probe #60 for *GAPDH*). All reactions were performed in triplicate using the ABI 7500 Real-Time PCR system (Applied Biosystems). Cycling conditions were 2 min at 50°C and 10 min at 95°C, followed by 40 cycles of 15 s at 95°C and 60 s at 60°C. Real-time PCR data were analyzed by the SDS version 1.2.1 software (Applied Biosystems). We evaluated the relative level of *RNF213* mRNA by determining the C_T value, the PCR cycle at which the reporter fluorescence exceeded the signal baseline. *GAPDH* mRNA was used as an internal reference for normalization of the quantitative expression values.

Multiplex PCR

MTC Multiple Tissue cDNA Panels (Clontech) were the source of human cell lines and cDNAs from human adult and fetal tissues. Multiplex PCRs were performed in a final volume of 20 µl using the Multiplex PCR Master Mix (Qiagen), 2 µl of cDNA, a 2 µM concentration of *RNF213* and a 10 µM concentration of *GAPDH*-specific primers. The samples were separated on a 2% agarose gel stained with ethidium bromide. Cycling conditions were 15 min at 94°C, followed by 30 cycles of 30 s at 94 °C, 30 s at 57 °C and 30 s at 72 °C. For normalization of the expression levels, we used *GAPDH* as an internal reference for each sample.

In situ hybridization (ISH) analysis

Paraffin-embedded blocks and sections of mouse tissues for ISH were obtained from Genostaff (Tokyo, Japan). The mouse tissues were dissected, fixed with Tissue Fixative (Genostaff), embedded in paraffin by proprietary procedures (Genostaff) and sectioned at 6 µm. To generate anti-sense and sense RNA probes, a 521-bp DNA fragment corresponding to nucleotide positions 470–990 of mouse *Rnf213* (BC038025) was subcloned into the pGEM-T Easy vector (Promega, Madison, WI, USA). Hybridization was performed with digoxigenin-labeled RNA probes at concentrations of 300 ng ml^{-1} in Probe Diluent-1 (Genostaff) at 60 °C for 16 h. Coloring reactions were performed with NBT/BCIP solution (Sigma-Aldrich, St Louis, MO, USA). The sections were counterstained with Kernechtrot stain solution (Mutoh, Tokyo, Japan), dehydrated and mounted with Malinol (Mutoh). For observation of *Rnf213* expression in activated lymphocytes, 10-week-old Balb/c mice were intraperitoneally injected with 100 µg of keyhole limpet hemocyanin and incomplete adjuvant and sacrificed in 2 weeks. The spleen of the mice was removed for Hematoxylin–eosin staining and ISH analyses.

RESULTS

Using 20 Japanese MMD families, we reevaluated the linkage mapped previously to five putative MMD loci. No locus with significant linkage, Lod score >3.0 or NPL score >4.0 was confirmed (Supplementary Figure 2). We conducted a genome-wide association study of 72 Japanese MMD cases. Single-marker allelic tests comparing the 72 MMD cases and 45 controls were performed for 785 720 SNPs using χ^2 statistics. These tests identified a single locus with a strong association with MMD ($P<10^{-8}$) on chromosome 17q25-ter (Figure 1b), which is in line with the latest mapping data of a MMD locus.[16] The SNP markers with $P<10^{-6}$ are listed in Table 1. To confirm this observation, we performed a locus-specific association study. A total of 384 SNP markers (Supplementary Table 1) were selected within the chromosome 17q25-ter region and genotyped in a set of 63 MMD cases and 45 controls. The SNP markers demonstrating a high association with MMD ($P<10^{-6}$) were clustered in a 151-kb region from base position 75 851 399–76 003 020 (SNP No.116–136 in

Table 1 A genome-wide association study of Japanese MMD patients and controls

	SNP	*Chromosome*	*Base position*	*Gene*	*Risk allele/ non-risk allele*	*Risk allele frequency in MMD*	*Risk allele frequency in controls*	χ^2	*P-value*	*Odds ratio*	*95% confidence interval*	
											Lower	*Upper*
1	rs11870849	17	76 025 668	*RNF213*	T/C	0.4792	0.1111	33.55	6.95E-09	7.36	3.532	15.34
2	rs6565681	17	75 963 089	*RNF213*	A/G	0.7361	0.3667	31.35	2.16E-08	4.819	2.733	8.489
3	rs7216493	17	75 941 953	*RNF213*	G/A	0.75	0.3889	30.39	3.53E-08	4.715	2.673	8.313
4	rs7217421	17	75 850 055	*RNF213*	A/G	0.6667	0.3	29.86	4.64E-08	4.666	2.642	8.237
5	rs12449863	17	75 857 806	*RNF213*	C/T	0.6667	0.3	29.86	4.64E-08	4.666	2.642	8.237
6	rs4890009	17	75 926 103	*RNF213*	G/A	0.8819	0.5778	28.5	9.38E-08	5.459	2.831	10.527
7	SNP17-75933731	17	75 933 731	*RNF213*	G/A	0.8819	0.5778	28.5	9.38E-08	5.458	2.831	10.527
8	rs7219131	17	75 867 365	*RNF213*	T/C	0.6667	0.3111	28.11	1.15E-07	4.429	2.517	7.794
9	rs6565677	17	75 932 037	*RNF213*	T/C	0.7431	0.3977	27.43	1.63E-07	4.378	2.483	7.722
10	rs4889848	17	75 969 256	*RNF213*	C/T	0.75	0.4111	26.99	2.05E-07	4.297	2.444	7.889
11	rs7224239	17	75 969 771	*RNF213*	A/G	0.8681	0.5667	26.99	2.05E-07	5.03	2.659	9.529

Abbreviations: MMD, moyamoya disease; SNP, single-nucleotide polymorphism.A genome-wide association study testing 1 140 419 SNPs on the Human Omni-Quad 1chip (Illumina, San Diego, CA, USA) was performed in 72 Japanese MMD cases. Single-marker allelic tests between the cases and controls were performed using χ^2 statistics for all markers. This table lists the 11 SNP markers with a significance of $P<10^{-6}$.

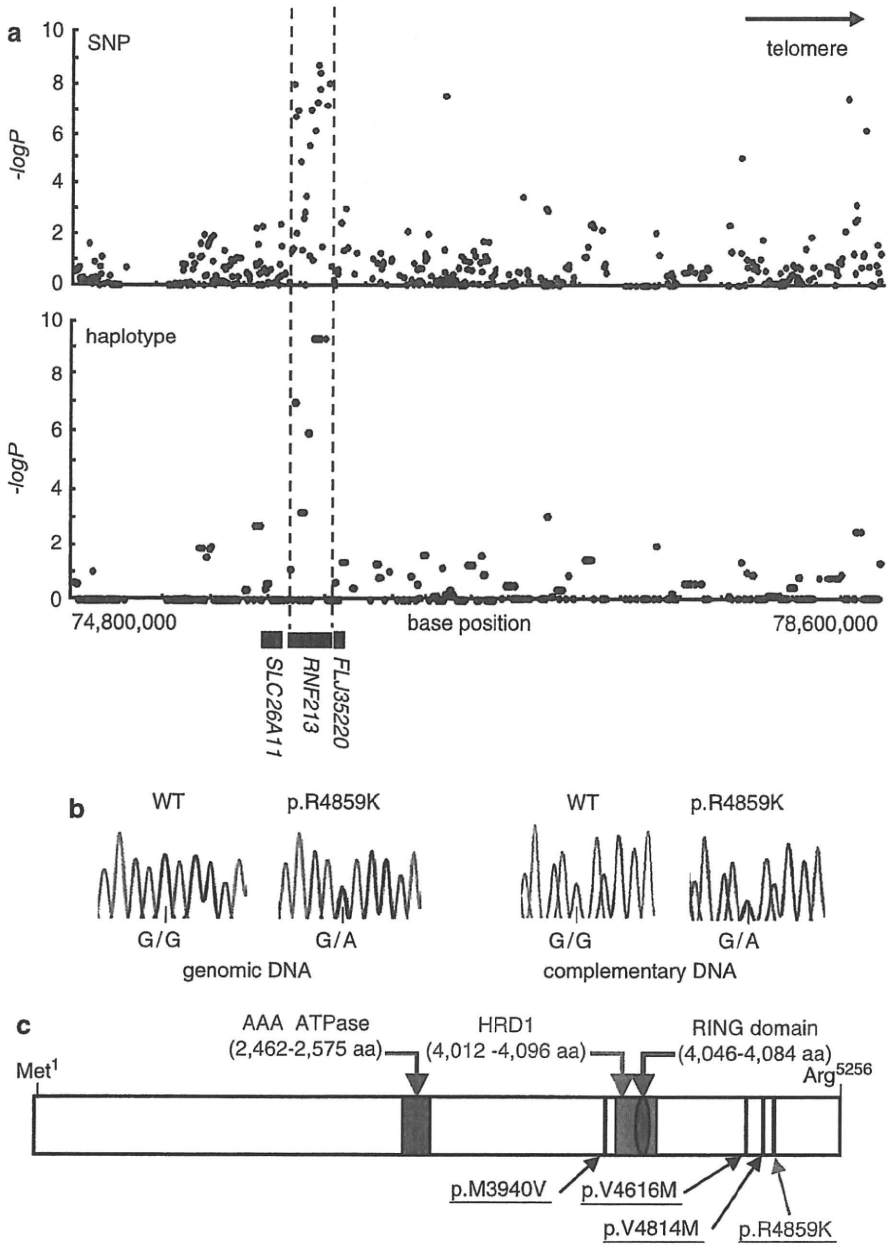

Figure 2 (**a**) Association analysis of 63 non-familial MMD cases and 45 control subjects. Statistical significance was evaluated by the χ^2-test. SNP markers with a strong association with MMD ($P<10^{-6}$) clustered in a 161-kb region (base position 75 851 399–76 012 838) indicated by two dotted lines (upper panel), which included the entire region of *RNF213* (lower panel). Haplotype analysis revealed a strong association ($P=5.3\times10^{-10}$) between MMD and a single haplotype located within *RNF213*. (**b**) Sequencing chromatograms of the identified MMD mutations. The left panel shows the sequences of an unaffected individual and a carrier of a p.R4859K heterozygous mutation. The right panel indicates the sequencing chromatograms of the leukocyte cDNA obtained from an unaffected individual and an individual with MMD who carries the p.R4859K mutation. Note that both wild-type and mutant alleles were expressed in leukocytes. (**c**) The structure of the RNF213 protein. The RNF213 protein contains three characteristic structures, the AAA-superfamily ATPase motif, the RING motif and the HMG-CoA reductase degradation motif. The positions of four mutations identified in MMD patients are underlined, including one prevalent mutation (red) and three private mutations (black).

Supplementary Table 1); this entire region was within the *RNF213* locus (Figure 2a). A single haplotype determined by seven SNPs (SNP Nos.130–136 in Supplementary Table 1) that resided in the 3′ region of *RNF213* was strongly associated with MMD onset ($P=5.3\times10^{-10}$). Analysis of the linkage disequilibrium block indicated that this haplotype was not in complete linkage disequilibrium with any other haplotype in this region (Supplementary Figure 3). These results strongly suggest that a founder mutation may exist in the 3′ part of *RNF213*.

Mutational analysis of the entire coding and promoter regions of *RNF213* and *FLJ35220*, a gene 3′ adjacent to *RNF213*, revealed that 19 of the 20 MMD families shared the same single base substitution, c.14576G>A, in exon 60 of *RNF213* (Figure 2b and Table 2). This nucleotide change causes an amino-acid substitution from arginine^{4859} to lysine^{4859} (p.R4859K). The p.R4859K mutation was identified in 46 of 63 non-familial MMD cases (73%), including 45 heterozygotes and a single homozygote (Table 3). Both the wild-type and the p.R4859K mutant alleles were co-expressed in leukocytes

Table 2 Nucleotide changes with amino-acid substitutions identified in the sequencing analysis of *RNF213* and *FLJ35220*

			Genotype (allele)				
Gene	*Exon*	*Nucleotide change[a] (amino-acid substitution)*	*Non-familial cases*	*Control subjects*	*P-value[b]*	*χ^2 (df=1) [c]*	*Odds ratio (95% CI)*
RNF213	29	c.7809C>A (p.D2603E)	2/63 (2/126)	15/381 (15/762)	0.77	0.09	0.80 (0.2–3.6)
RNF213	41	c.11818A>G (p.M3940V)	1/63 (1/126)	0/388 (0/776)	0.01	6.17	ND
RNF213	41	c.11891A>G (p.E3964G)	4/63 (4/126)	3/55 (4/110)	0.84	0.04	1.2 (0.3–5.5)
RNF213	52	c.13342G>A (p.A4448T)	4/63 (4/126)	2/53 (2/106)	0.53	0.39	1.7 (0.3–9.8)
RNF213	56	c.13846G>A (p.V4616M)	1/63 (1/126)	0/388 (0/776)	0.01	6.17	ND
RNF213	59	c.14440G>A (p.V4814M)	1/63 (1/126)	0/388 (0/776)	0.01	6.17	ND
RNF213	60	c.14576G>A (p.R4859K)	46/63 (47/126)	6/429 (6/858)	1.2×10^{-43}	298.1	190.8 (71.7–507.9)
FLJ35220		None					

Abbreviations: ND, not determined; SNP, single-nucleotide polymorphism.
[a]Nucleotide numbers of *RNF213* cDNA are counted from the A of the ATG initiator methionine codon (NCBI Reference sequence, NP_065965.4).
[b]*P*-values were calculated by Fisher's exact test.
[c]Genotypic distribution (carrier of the polymorphism vs non-carrier).

Table 3 Association of the p.R4859K (c.14576G>A) mutation with MMD

		Genotype		
	Total	*wt/wt (%)*	*wt/p.R4859K (%)*	*p.R4859K/ p.R4859K (%)[d]*
Members of 19 MMD families[a]				
Affected	42	0	39 (92.9)	3 (7.1)
Not affected	28	15 (53.6)	13 (46.4)	0
Individuals without a family history of MMD[b,c]				
Affected	63	17 (27.0)	45 (71.4)	1 (1.6)
Not affected	429	423 (98.6)	6 (1.4)	0

Abbreviations: MMD, moyamoya disease.
[a]Entire distribution, $\chi^2=29.4$, $P=4.2\times10^{-7}$.
[b]Entire distribution, $\chi^2=298.2$, $P=1.8\times10^{-65}$.
[c]Genotypic distribution (p.R4859K carrier vs non-carrier), $\chi^2=298.1$, $P=1.2\times10^{-43}$, odds ratio=190.8 (95% CI=71.7–507.9).
[d]The age of onset and initial symptoms of the four homozygotes were comparable to those of the 84 heterozygous patients.

in three patients heterozygous for the p.R4859K mutation (Figure 2b), excluding the possible instability of the mutant *RNF213* mRNA. Additional missense mutations, p.M3940V, p.V4616M and p.V4814M, were detected in three non-familial MMD cases without the p.R4859K mutation (Figure 2c). These mutations were not found in 388 control subjects and were detected in only one patient, suggesting that they were private mutations (Table 2). No copy number variation or mutation was identified in the *RNF213* locus of 12 MMD patients using comparative genome hybridization microarray analysis (Supplementary Figure 4). In total, 6 of the 429 control subjects (1.4%) were found to be heterozygous carriers of p.R4859K. Therefore, we concluded that the p.R4859K mutation increases the risk of MMD by a remarkably high amount (odds ratio=190.8 (95% confidence interval=71.7–507.9), $P=1.2\times10^{-43}$) (Table 3). It was recently reported that an SNP (ss161110142) in the promoter region of *RPTOR*, which is located ~150 kb downstream from *RNF213*, was associated with MMD.[17] Genotyping of the SNP in *RPTOR* showed that the *RNF213* p.R4859K mutation was more strongly associated with MMD than ss161110142 (Supplementary Figure 1).

RNF213 encodes a protein with 5256 amino acids harboring a RING (really interesting new gene) finger motif, suggesting that it functions as an E3 ubiquitin ligase (Figure 2c). It also has an AAA ATPase domain, which is characteristic of energy-dependent unfoldases.[18] To our knowledge, RNF213 is the first RING finger protein known to contain an AAA ATPase domain. The expression profile of *RNF213* has not been previously fully characterized. We performed a quantitative reverse transcription PCR analysis in various human tissues and cells. *RNF213* mRNA was highly expressed in immune tissues, such as spleen and leukocytes (Figure 3a and Supplementary Figure 5). Expression of *RNF213* was detected in fractions of both polymorphonuclear cells and mononuclear cells and was found in both B and T cell fractions (Supplementary Figure 6). A low but significant expression of *RNF213* was also observed in human umbilical vein endothelial cells and human pulmonary artery smooth muscle cells. Cellular expression was not enhanced in tumor cell lines, compared with leukocytes. In human fetal tissues, the highest expression was observed in leukocytes and the thymus (Supplementary Figure 6E). The expression of *RNF213* was surprisingly low in both adult and fetal brains. Overall, *RNF213* was ubiquitously expressed, and the highest expression was observed in immune tissues.

We studied the cellular expression of *Rnf213* in mice. The ISH analysis of spleen showed that *Rnf213* mRNA was present in small mononuclear cells, which were mainly localized in the white pulps (Figures 3b–g). The ISH signals were also detected in the primary follicles in the lymph node and in thymocytes in the medulla of the thymus (Supplementary Figure 7). To study *Rnf213* expression in activated lymphocytes we immunized mice with keyhole limpet hemocyanin, and examined *Rnf213* mRNA in spleen by ISH analysis. Primary immunization with keyhole limpet hemocyanin antigen revealed that the expression of *Rnf213* in the secondary follicle is as high as in the primary follicle in the lymph node (Supplementary Figure 8). In an E16.5 mouse embryo, expression was observed in the medulla of the thymus and in the cells around the mucous palatine glands (Supplementary Figure 9). These findings suggest that mature lymphocytes in a static state express *Rnf213* mRNA at a higher level than do their immature counterparts.

DISCUSSION

We identified a susceptibility locus for MMD by genome-wide and locus-specific association studies. Further sequencing analysis revealed a founder missense mutation in *RNF213*, p.R4859K, which was tightly associated with MMD onset. Identification of a founder mutation in individuals with MMD would resolve the following recurrent

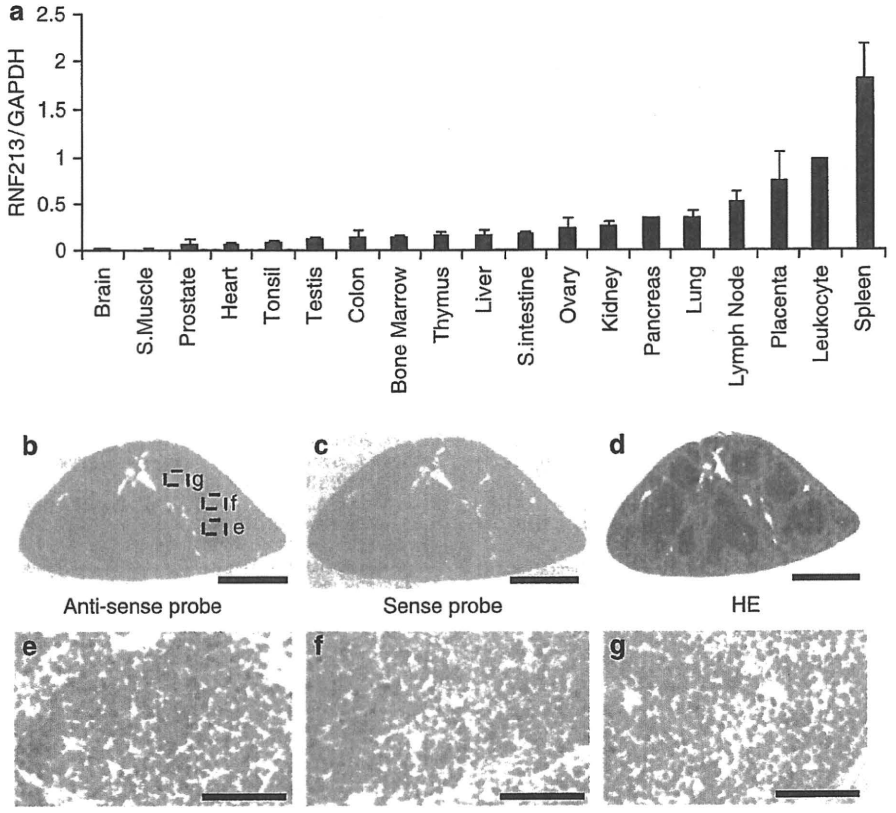

Figure 3 Expression of human RNF213 and murine Rnf213. (**a**) RT-PCR analysis of RNF213 mRNA in various human tissues. The expression levels of *RNF213* mRNA in various adult human tissues were evaluated by quantitative PCR using *GAPDH* mRNA as a control. The signal ratio of *RNF213* mRNA to *GAPDH* mRNA in each sample is shown on the vertical axis. (**b–g**) *In situ* hybridization (ISH) analysis of Rnf213 mRNA in mouse spleen. Specific signals for *Rnf213* mRNA were detected by ISH analysis with the anti-sense probe (**b**) but not with the sense probe (**c**). Hematoxylin–eosin staining of the mouse spleen (**d**). Signals for the *Rnf213* mRNA were observed in small mononuclear cells, which were mainly localized in the white pulps (dotted square, **e**) and partially distributed in the red pulps (dotted squares, **f** and **g**). Panels e, f and g show the high-magnification images of the corresponding fields in panel b. Scale bars, 1 mm (**b–d**) and 50 μm (**e–g**).

questions:[2,19] (i) why is MMD more prevalent in East Asia than in Western countries? The carrier frequency of p.R4859K in Japan is 1/72 (Table 2). In contrast, we found no p.R4859K carrier in 400 Caucasian controls (data not shown). Furthermore, no mutation was identified in five Caucasian patients with MMD after the full sequencing of *RNF213*. These results suggest that the genetic background of MMD in Asian populations is distinct from that in Western populations and that the low incidence of MMD in Western countries may be attributable to a lack of the founder *RNF213* mutation. (ii) Is unilateral involvement a subtype of MMD or a different disease?[2] We collected DNA samples from six patients with unilateral involvement and found a p.R4859K mutation in four of them (data not shown), suggesting that bilateral and unilateral MMD share a genetic background. (iii) Is pre-symptomatic diagnosis of MMD possible? In the present study, MMD never developed in the 15 mutation-negative family members in the 19 MMD families with the p.R4859K mutation (Table 3 and Supplementary Figure 1), suggesting the feasibility of presymptomatic diagnosis or exclusion by genetic testing.

How the mutant RNF213 protein causes MMD remains to be elucidated. The expression of *RNF213* was more abundant in a subset of leukocytes than in the brain, suggesting that blood cells have a function in the etiology of MMD. This observation agrees with a previous report that MMD patients have systemic angiopathy.[20] Recent studies have suggested that the postnatal vasculature can form through vasculogenesis, a process by which endothelial progenitor cell are recruited from the splenic pool and differentiate into mature endothelial cells.[21] Levels of endothelial progenitor cells in the peripheral blood are increased in MMD patients.[22] *RNF213* may be expressed in splenic endothelial progenitor cells and mutant *RNF213* might dysregulate the function of the endothelial progenitor cells. Further research is necessary to elucidate the role of *RNF213* in the etiology of MMD.

CONFLICT OF INTEREST

The authors declare no conflict of interest.

ACKNOWLEDGEMENTS

We thank all of the patients and their families for participating in this study. We also thank Dr Hidetoshi Ikeda at the Department of Neurosurgery, Tohoku University School of Medicine and Drs Toshiaki Hayashi and Reizo Shirane at the Department of Neurosurgery, Miyagi Children's Hospital, Sendai, Japan for patient recruitment. We are grateful to Ms Kumi Kato for technical assistance. This study was supported by grants from the Ministry of Education, Culture, Sports, Science and Technology, Japan and by the Research Committee on Moyamoya Disease of the Ministry of Health, Labor and Welfare, Japan.

1 Suzuki, J. & Takaku, A. Cerebrovascular 'moyamoya' disease. Disease showing abnormal net-like vessels in base of brain. *Arch. Neurol.* **20,** 288–299 (1969).
2 Suzuki, J. *Moyamoya Disease* (Springer-Verlag: Berlin, 1983).
3 Oki, K., Hoshino, H. & Suzuki, N. In: *Moyamoya Disease Update*, (eds Cho B.K., Tominaga T.) 29–34 (Springer: New York, 2010).
4 Phi, J. H., Kim, S. K., Wang, K. C. & Cho, B. K. In: *Moyamoya Disease Update*, (eds Cho B.K., Tominaga T). 82–86, (Springer: New York, 2010).
5 Yoshihara, T., Taguchi, A., Matsuyama, T., Shimizu, Y., Kikuchi-Taura, A., Soma, T. *et al.* Increase in circulating CD34-positive cells in patients with angiographic evidence of moyamoya-like vessels. *J. Cereb. Blood Flow Metab.* **28,** 1086–1089 (2008).
6 Achrol, A. S., Guzman, R., Lee, M. & Steinberg, G. K. Pathophysiology and genetic factors in moyamoya disease. *Neurosurg. Focus.* **26,** E4 (2009).
7 Scott, R. M. & Smith, E. R. Moyamoya disease and moyamoya syndrome.. *N. Engl. J. Med.* **360,** 1226–1237 (2009).
8 Kure, S. In: *Moyamoya Disease Update* (eds Cho B.K., Tominaga T.) 41–45 (Springer: Tokyo, 2010).
9 Kuriyama, S., Kusaka, Y., Fujimura, M., Wakai, K., Tamakoshi, A., Hashimoto, S. *et al.* Prevalence and clinicoepidemiological features of moyamoya disease in Japan: findings from a nationwide epidemiological survey. *Stroke.* **39,** 42–47 (2008).
10 Sakurai, K., Horiuchi, Y., Ikeda, H., Ikezaki, K., Yoshimoto, T., Fukui, M. *et al.* A novel susceptibility locus for moyamoya disease on chromosome 8q23. *J. Hum. Genet.* **49,** 278–281 (2004).
11 Nanba, R., Kuroda, S., Tada, M., Ishikawa, T., Houkin, K. & Iwasaki, Y. Clinical features of familial moyamoya disease. *Childs. Nerv. Syst.* **22,** 258–262 (2006).
12 Ikeda, H., Sasaki, T., Yoshimoto, T., Fukui, M. & Arinami, T. Mapping of a familial moyamoya disease gene to chromosome 3p24.2-p26. *Am. J. Hum. Genet.* **64,** 533–537 (1999).
13 Inoue, T. K., Ikezaki, K., Sasazuki, T., Matsushima, T. & Fukui, M. Linkage analysis of moyamoya disease on chromosome 6. *J. Child. Neurol.* **15,** 179–182 (2000).
14 Yamauchi, T., Tada, M., Houkin, K., Tanaka, T., Nakamura, Y., Kuroda, S. *et al.* Linkage of familial moyamoya disease (spontaneous occlusion of the circle of Willis) to chromosome 17q25.. *Stroke.* **31,** 930–935 (2000).
15 Wakai, K., Tamakoshi, A., Ikezaki, K., Fukui, M., Kawamura, T., Aoki, R. *et al.* Epidemiological features of moyamoya disease in Japan: findings from a nationwide survey. *Clin. Neurol. Neurosurg.* **99**(Suppl 2), S1–S5 (1997).
16 Mineharu, Y., Liu, W., Inoue, K., Matsuura, N., Inoue, S., Takenaka, K. *et al.* Autosomal dominant moyamoya disease maps to chromosome 17q25.3. *Neurology.* **70,** 2357–2363 (2008).
17 Liu, W., Hashikata, H., Inoue, K., Matsuura, N., Mineharu, Y., Kobayashi, H. *et al.* A rare Asian founder polymorphism of Raptor may explain the high prevalence of Moyamoya disease among East Asians and its low prevalence among Caucasians. *Environ. Health. Prev. Med.* **15,** 94–104 (2010).
18 Lupas, A. N. & Martin, J. AAA proteins.. *Curr. Opin. Struct. Biol.* **12,** 746–753 (2002).
19 Ikezaki, K. In: *Moyamoya disease* (eds Ikezaki K., Loftus C. M.) 43–75 (Thieme: New York, 2001).
20 Ikeda, E. Systemic vascular changes in spontaneous occlusion of the circle of Willis. *Stroke.* **22,** 1358–1362 (1991).
21 Zampetaki, A., Kirton, J. P. & Xu, Q. Vascular repair by endothelial progenitor cells. *Cardiovasc. Res.* **78,** 413–421 (2008).
22 Rafat, N., Beck, G., Pena-Tapia, P. G., Schmiedek, P. & Vajkoczy, P. Increased levels of circulating endothelial progenitor cells in patients with Moyamoya disease. *Stroke.* **40,** 432–438 (2009).

Supplementary Information accompanies the paper on Journal of Human Genetics website (http://www.nature.com/jhg)

Human Molecular Genetics, 2010, Vol. 19, No. 14 **2898–2906**
doi:10.1093/hmg/ddq176
Advance Access published on April 27, 2010

Common variants in *CASP3* confer susceptibility to Kawasaki disease

Yoshihiro Onouchi[1,*], Kouichi Ozaki[1], Jane C. Buns[2,3,25], Chisato Shimizu[2,3,25], Hiromichi Hamada[4], Takafumi Honda[4], Masaru Terai[4], Akihito Honda[5], Takashi Takeuchi[6], Shoichi Shibuta[6], Tomohiro Suenaga[6], Hiroyuki Suzuki[6], Kouji Higashi[7], Kumi Yasukawa[7], Yoichi Suzuki[8], Kumiko Sasago[8], Yasushi Kemmotsu[9], Shinichi Takatsuki[9], Tsutomu Saji[9], Tetsushi Yoshikawa[10], Toshiro Nagai[11], Kunihiro Hamamoto[12], Fumio Kishi[13], Kazunobu Ouchi[14], Yoshitake Sato[15], Jane W. Newburger[16,25], Annette L. Baker[16,25], Stanford T. Shulman[17,25], Anne H. Rowley[17,25], Mayumi Yashiro[18], Yoshikazu Nakamura[18], Keiko Wakui[19], Yoshimitsu Fukushima[19], Akihiro Fujino[20], Tatsuhiko Tsunoda[21], Tomisaku Kawasaki[22], Akira Hata[8], Yusuke Nakamura[23,24] and Toshihiro Tanaka[1]

[1]Laboratory for Cardiovascular diseases, Center for Genomic Medicine RIKEN, Yokohama 230-0045, Japan, [2]Department of Pediatrics, School of Medicine, University of California San Diego, La Jolla, CA, USA, [3]Rady Children's Hospital San Diego, CA 92093-0641, USA, [4]Department of Pediatrics, Tokyo Women's Medical University Yachiyo Medical Center, Yachiyo 276-8524, Japan, [5]Department of Pediatrics, Asahi General Hospital, Asahi 289-2511, Japan, [6]Department of Pediatrics, Wakayama Medical University, Wakayama 641-0012, Japan, [7]Department of Pediatrics and [8]Department of Public Health, Chiba University Graduate School of Medicine, Chiba 260-8670, Japan, [9]Department of Pediatrics, Toho University School of Medicine, Tokyo 143-8541, Japan, [10]Department of Pediatrics, Fujita Health University, Toyoake 470-1192, Japan, [11]Department of Pediatrics, Dokkyo Medical University, Koshigaya Hospital, Koshigaya 343-8555, Japan, [12]Department of Speech and Hearing Sciences, International University of health and welfare, Fukuoka 831-8501, Japan, [13]Department of Molecular Genetics and [14]Department of Pediatrics, Kawasaki Medical School, Kurashiki 701-0192, Japan, [15]Department of Pediatrics, Fuji Heavy Industry LTD, Health Insurance Society General Ohta Hospital, Ohta 373-8585, Japan, [16]Department of Cardiology, Boston Children's Hospital, Boston, MA 02115, USA, [17]Department of Pediatrics, Feinberg School of Medicine Northwestern University, Children's Memorial Hospital, Chicago, IL 60611, USA, [18]Department of Public Health, Jichi Medical School, Minamikawachi 329-0498, Japan, [19]Department of Preventive Medicine, Shinshu University School of Medicine, Matsumoto 390-8621, Japan, [20]Department of Surgery, National Center for Child Health and Development, Tokyo 157-8535, Japan, [21]Laboratory for Medical Informatics, Center for Genomic Medicine, RIKEN, Yokohama 230-0045, Japan, [22]Japan Kawasaki Disease Research Center, Tokyo 101-0041, Japan, [23]Laboratory for Molecular Medicine, Human Genome Center, Institute of Medical Science, University of Tokyo, Tokyo 108-8639, Japan, [24]Center for Genomic Medicine RIKEN, Yokohama 230-0045, Japan and [25]U. S. KD Genetics Consortium

Received January 19, 2010; Revised and Accepted April 23, 2010

Kawasaki disease (KD; OMIM 611775) is an acute vasculitis syndrome which predominantly affects small- and medium-sized arteries of infants and children. Epidemiological data suggest that host genetics underlie the disease pathogenesis. Here we report that multiple variants in the caspase-3 gene (*CASP3*) that are in linkage disequilibrium confer susceptibility to KD in both Japanese and US subjects of European ancestry. We found that a G to A substitution of one commonly associated SNP located in the 5′ untranslated region of *CASP3* (rs72689236; $P = 4.2 \times 10^{-8}$ in the Japanese and $P = 3.7 \times 10^{-3}$ in the European Americans) abolished

*To whom correspondence should be addressed. Tel: +81 455039347; Fax: +81 455039289; Email: onouchi@src.riken.jp

binding of nuclear factor of activated T cells to the DNA sequence surrounding the SNP. Our findings suggest that altered *CASP3* expression in immune effecter cells influences susceptibility to KD.

INTRODUCTION

Kawasaki disease (KD) is characterized by high fever, polymorphous skin rash, injection of the conjunctiva, erythema of the palms and soles followed by desquamation, redness of oral mucosa and lips and non-supprative cervical lymphadenopathy (1,2). Despite clinical and epidemiological features suggesting an infectious trigger in the pathogenesis of KD, the etiology remains unknown. Marked activation of the immune system accompanied by infiltration of lymphocytes, macrophages and neutrophils into the vascular wall occurs during the acute phase of KD. The coronary arteries are selectively targeted and coronary artery lesions (CALs) develop in 20–25% of the patients without treatment (3). KD is now a leading cause of acquired cardiac disease in children in developed countries.

Previously, we performed an affected sibpair linkage study and identified several candidate regions (4q35, 5q31.4, 6q27, 7p15, 8q24, 12q24, 18q23, 19q13.2, Xp12 and Xq26) for KD susceptibility (4). Recently, we identified a functional SNP in *ITPKC*, encoding inositol 1,4,5-trisphosphate 3 kinase-C on 19q13.2, that confers both increased risk of KD and CAL formation (5). This effect is likely mediated through upregulating of the Ca^{2+}/NFAT pathway in T cells, thus increasing IL-2 production. These findings supported the hypothesis that genetically determined modulation of the immune response is fundamental to KD pathogenesis and suggested that genes with immune regulatory function located in chromosomal regions with positive linkage signals should be considered potential candidates for KD susceptibility. In an attempt to identify a novel susceptibility gene, we performed a positional candidate gene study for 4q35 region. We found that there is a set of common variants in *caspase-3* (*CASP3*) gene significantly associated with KD in both Japanese and European American subjects. We also demonstrate a functional significance of one commonly associated SNP which affects binding of nuclear factor of activated T cells (NFAT) to the 5′ untranslated region (UTR) of the gene.

RESULTS

Identification of the variants of *CASP3* gene associated with KD susceptibility

The candidate region on 4q35 was attractive because several immune genes have been mapped around the peak of linkage, including the interferon regulatory factor 2 gene (*IRF2*), *CASP3* and toll-like receptor 3 gene (*TLR3*), which all lie within 1.7 Mb of the linkage peak. Previous reports describing delayed apoptosis of peripheral blood lymphocytes (6) and neutrophils (7) from KD patients led us to focus on *CASP3*, which is located at 185.8 Mb on chromosome 4 close to the linkage peak (184.9 Mb). Caspase-3 is a key molecule of activation-induced cell death (AICD) (8) and it has also been reported to cleave the inositol 1,4,5-triphosphate receptor, Type 1 (ITPR1) in apoptotic T cells. ITPR1 is a receptor for inositol 1,4,5-trisphosphate (IP3), a substrate for ITPKC in T cells (9).

Based on linkage disequilibrium (LD) data at the web site of the International HapMap project, we selected 12 tagging SNPs with minor allele frequency (MAF) greater than 5% from the 36 kb region containing the *CASP3* gene flanked by 10 kb upstream and 5 kb downstream (Supplementary Material, Fig. S1). Using Haploview 4.1, the tagging SNPs were classified into four SNP groups at a threshold of $r^2 > 0.8$. Four tagging SNPs (rs4647693, rs2696057, rs2720378 and rs2705881) were selected as representatives of each group (Supplementary Material, Fig. S1). For the first stage of screening, the genotype at these four locations was determined for 638 Japanese KD patients and 1031 healthy Japanese controls. Three SNPs showed significant association with KD ($P < 0.05$ after Bonferroni correction for four tests; Supplementary Material, Fig. S1) when comparing allele frequencies between cases and controls. We then resequenced the 36 kb region in 24 Japanese subjects (12 KD subjects and 12 controls) and genotyped the first case–control panel for 34 additional variants and compared allele frequencies (Supplementary Material, Table S1). Twenty-five of the 46 variants (12 tagging SNPs + 34 additional variants) showed P-values < 0.001 ($P < 0.05$ after a conservative Bonferroni correction for 46 tests) and most were clustered in the 5′ region of *CASP3* (Fig. 1). To validate the association and identify of the causative variant, these 25 loci were further examined in an independent Japanese case–control panel with 282 KD patients and 378 controls. In this case–control panel, all of the 25 variants showed the same trend of association and rs2720378 was the most significant in a meta-analysis by the Mantel–Haenszel method [odds ratio (OR) = 1.44, 95% confidence interval (CI) 1.27–1.62; $P = 3.5 \times 10^{-9}$; Table 1]. Most of the 25 significant variants except for rs4862399 and rs7693625 were in high linkage disequilibrium with rs2720378 ($r^2 > 0.69$) and showed the same trend of association. No increase of association due to haplotypic effect was seen for the combination of rs2720378 and any other variations including rs4862399 and rs7693625 in a haplotype association study and logistic regression analysis (Supplementary Material, Tables S2 and S3).

Screening of functionally significant variants

We next assessed the functional significance of the variants in *CASP3*. Because all of the 25 variants were in untranscribed or untranslated of *CASP3*, we postulated that the variant(s) might influence expression of *CASP3*. We screened for possible enhancer activity around the associated variants by a reporter gene assay. To facilitate the screening, we cloned four tandem copies of oligonucleotides corresponding to both alleles of the variants upstream of the SV40 promoter in the luciferase reporter vector, pGL3, and transfected them into Jurkat cells.

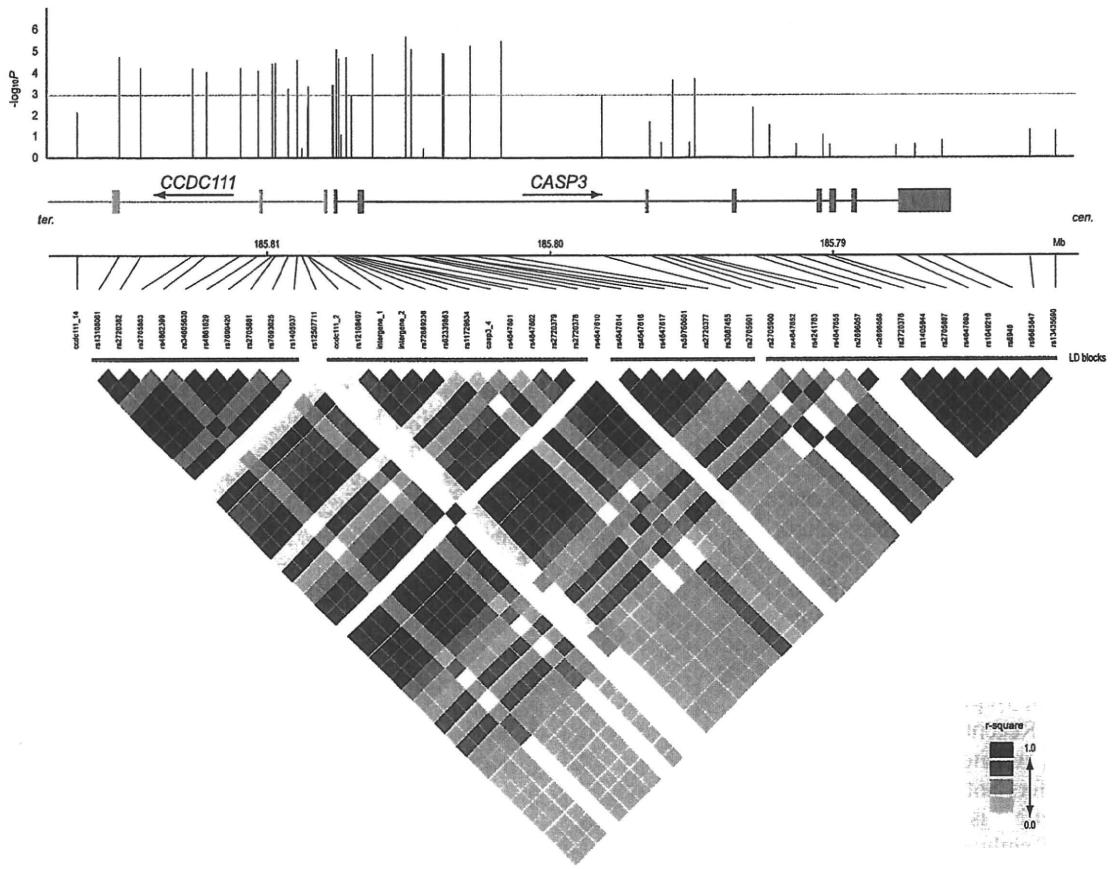

Figure 1. Linkage disequilibrium (LD) structure of the *CASP3* locus and association of the variants with KD in Japanese subjects. Pairwise LD plots with 46 variants distributed across the 36 kb region in and surrounding *CASP3* are illustrated using Haploview software. Values for r^2 were calculated using genotype data from Japanese control samples ($n = 1031$). Blue horizontal bars under SNP IDs represent LD blocks defined by Gabriel's rule. The genomic organization of *CASP3* and the coiled-coil domain containing 111 (*CCDC111*; only 5′ part is shown) is illustrated with blue and gray boxes representing the exons. Arrows under the gene names indicate the orientation of transcription. The position and the negative log of the *P*-values from the genetic association study (637 KD cases and 1031 controls; allelic frequency comparison) for each variant tested are shown by vertical bars in the upper panel. Threshold for statistical significance ($P = 0.001$) was indicated by a gray horizontal line in the upper panel.

In this screening, we found that the sequence surrounding rs72689236 located in the 5′-UTR of *CASP3* showed an enhancer activity which was significantly lower for the risk allele (A) compared with the protective allele (G) (Fig. 2A). We also found that the allelic difference was more prominent when these plasmids were transfected into peripheral blood mononuclear cells (PBMCs) or $CD3^+$ T cells. In contrast, the difference was modest when transfected into HeLa cells (data not shown). Enhancement of luciferase activity was also observed when the plasmids corresponding to intergene_1, rs62339863 and rs2720377 were transfected. However, there was no significant difference between either allele of these three SNPs. Neither enhancer function nor allelic difference was detected for rs2720378, rs4647610, rs4647616, rs4647617 and rs59760601 (Supplementary Material, Fig. S2).

Rs72689236 affects binding of NFAT to the 5′-UTR of *CASP3*

To elucidate the enhancer element that may lie near rs72689236 further, we conducted an electrophoretic mobility shift assay (EMSA) using nuclear extract from PBMCs and rs72689236 oligonucleotides as probes. As shown in Figure 2D, there was a band shift using the probe specific to the G allele. Although no binding sequence of known transcription factor was predicted near rs72689236, we focused on the GGAA sequence of which the first 'G' is changed to 'A' by the SNP. Sequence similarity to the consensus binding sequence of NFAT (GGAAAA) and a recent publication describing relationship between NFAT and *CASP3* expression (10) led us to postulate NFAT as a candidate transactivator for this site. We tested this hypothesis by conducting further luciferase assay and EMSA. In luciferase assay, both NFATc1 and NFATc2 overexpressed in HeLa cells, which have lower endogenous levels of NFATs (11), significantly enhanced the difference (Supplementary Material, Fig. S3). In contrast, cyclosporin A, a calcineurin inhibitor which suppresses NFAT signaling, minimized the difference observed in Jurkat cells (Fig. 2B). While in EMSA, formation of a DNA–protein complex was abolished by cyclosporine A added in the culture medium of PBMCs from which nuclear protein was extracted, and was competed by excess amount of unlabeled oligonucleotide with an NFAT binding sequence

Table 1. Association of genetic variants in the region of *CASP3* and Kawasaki disease in two independent panels of Japanese subjects

Variants	Position[a]	Alleles[b] Major	Minor	Panel 1 ($n = 1669$) MAF KD ($n = 638$)	Control ($n = 1031$)	OR	95% CI	*P*-values	Panel 2 ($n = 660$) MAF KD ($n = 282$)	Control ($n = 378$)	OR	95% CI	*P*-values	Combined[c] OR	95% CI	*P*-values	r^2 with rs2720378
rs13108061	185815223	C	A	0.43	0.35	1.37	1.19–1.58	1.7×10^{-5}	0.41	0.34	1.36	1.09–1.71	6.9×10^{-3}	1.37	1.21–1.54	3.8×10^{-7}	0.79
rs2720382	185814464	A	T	0.44	0.37	1.34	1.16–1.54	5.8×10^{-5}	0.42	0.34	1.41	1.13–1.77	2.5×10^{-3}	1.36	1.21–1.53	5.3×10^{-7}	0.75
rs2705883	185812635	T	C	0.44	0.37	1.34	1.17–1.55	4.7×10^{-5}	0.42	0.34	1.41	1.13–1.77	2.5×10^{-3}	1.36	1.21–1.54	4.3×10^{-7}	0.75
rs4862399	185812136	T	C	0.26	0.20	1.39	1.18–1.64	8.4×10^{-5}	0.25	0.19	1.38	1.06–1.80	0.016	1.39	1.21–1.59	4.0×10^{-6}	0.36
rs34605630	185810931	T	C	0.44	0.37	1.34	1.16–1.54	6.6×10^{-5}	0.42	0.34	1.41	1.12–1.76	2.8×10^{-3}	1.36	1.20–1.53	6.7×10^{-7}	0.74
rs4861629	185810306	G	C	0.44	0.37	1.33	1.16–1.54	7.5×10^{-5}	0.42	0.34	1.41	1.12–1.76	2.9×10^{-3}	1.35	1.20–1.53	8.0×10^{-7}	0.74
rs7699420	185809818	G	A	0.44	0.37	1.35	1.17–1.55	4.3×10^{-5}	0.42	0.34	1.43	1.14–1.79	1.8×10^{-3}	1.37	1.21–1.54	3.0×10^{-7}	0.74
rs2705881	185809719	T	C	0.44	0.37	1.35	1.17–1.56	3.3×10^{-5}	0.42	0.34	1.41	1.12–1.76	3.1×10^{-3}	1.37	1.21–1.54	3.6×10^{-7}	0.75
rs7693625	185809252	T	C	0.26	0.21	1.34	1.14–1.58	4.7×10^{-4}	0.25	0.21	1.27	0.98–1.65	0.070	1.32	1.15–1.51	8.7×10^{-5}	0.34
rs1405937	185808932	G	C	0.43	0.36	1.36	1.18–1.57	2.5×10^{-5}	0.41	0.34	1.37	1.10–1.72	5.7×10^{-3}	1.36	1.21–1.54	4.7×10^{-7}	0.79
rs12108497	185808551	A	G	0.43	0.37	1.30	1.13–1.50	2.9×10^{-4}	0.41	0.33	1.42	1.13–1.78	2.4×10^{-3}	1.33	1.18–1.51	2.7×10^{-6}	0.78
Intergene_1	185807690	T	C	0.52	0.45	1.29	1.12–1.48	3.6×10^{-4}	0.52	0.39	1.69	1.36–2.11	2.7×10^{-6}	1.39	1.24–1.57	4.0×10^{-8}	0.69
Intergene_2	185807669	G	C	0.51	0.45	1.28	1.11–1.47	5.1×10^{-4}	0.52	0.39	1.66	1.33–2.07	6.3×10^{-6}	1.38	1.23–1.55	8.5×10^{-8}	0.70
rs72689236	185807547	G	A	0.46	0.38	1.38	1.20–1.59	7.2×10^{-6}	0.44	0.35	1.43	1.15–1.79	1.6×10^{-3}	1.40	1.24–1.57	4.2×10^{-8}	0.88
rs62339863	185807461	G	T	0.45	0.38	1.36	1.18–1.57	2.1×10^{-5}	0.44	0.34	1.53	1.22–1.92	2.0×10^{-4}	1.41	1.25–1.58	2.4×10^{-8}	0.91
casp3_4	185807195	–	G	0.46	0.38	1.36	1.18–1.57	2.1×10^{-5}	0.45	0.35	1.53	1.22–1.91	1.9×10^{-4}	1.41	1.25–1.58	2.3×10^{-8}	0.90
rs2720379	185806266	T	C	0.46	0.38	1.37	1.19–1.58	1.2×10^{-5}	0.44	0.34	1.53	1.22–1.91	2.0×10^{-4}	1.41	1.26–1.59	1.2×10^{-8}	0.92
rs2720378	185805107	C	G	0.45	0.36	1.41	1.22–1.63	2.0×10^{-6}	0.43	0.34	1.50	1.20–1.88	4.1×10^{-4}	1.44	1.27–1.62	3.5×10^{-9}	1.0
rs4647610	185804925	A	G	0.46	0.38	1.39	1.20–1.60	6.1×10^{-6}	0.44	0.34	1.53	1.22–1.91	0.00021	1.42	1.26–1.61	6.6×10^{-9}	0.94
rs4647616	185803825	A	G	0.45	0.38	1.37	1.19–1.57	1.5×10^{-5}	0.45	0.35	1.51	1.21–1.89	0.00028	1.41	1.25–1.59	2.1×10^{-8}	0.94
rs4647617	185803775	A	G	0.46	0.38	1.37	1.19–1.58	1.3×10^{-5}	0.45	0.34	1.53	1.22–1.91	0.00020	1.41	1.25–1.59	1.4×10^{-8}	0.94
rs59760601	185802837	T	C	0.46	0.38	1.38	1.20–1.59	8.7×10^{-6}	0.44	0.34	1.53	1.22–1.91	0.00020	1.42	1.26–1.60	9.1×10^{-9}	0.94
rs2720377	185801740	G	A	0.45	0.37	1.40	1.21–1.61	3.5×10^{-6}	0.43	0.34	1.48	1.18–1.85	0.00060	1.42	1.26–1.60	8.7×10^{-9}	0.99
rs4647652	185795678	T	C	0.43	0.37	1.31	1.14–1.51	2.1×10^{-4}	0.43	0.33	1.51	1.20–1.89	0.00034	1.36	1.21–1.54	4.5×10^{-7}	0.75
rs4647655	185794892–185794893	TTCAGGATTT	–	0.43	0.37	1.32	1.15–1.52	1.3×10^{-4}	0.42	0.33	1.44	1.15–1.52	0.0015	1.35	1.20–1.53	7.9×10^{-7}	0.75

[a]Positions of variants are based on Build 36.3 chromosome 4 reference sequence.
[b]Nucleotides of reverse strand are shown.
[c]Combined data analysis was conducted with Mantel–Haenszel method.

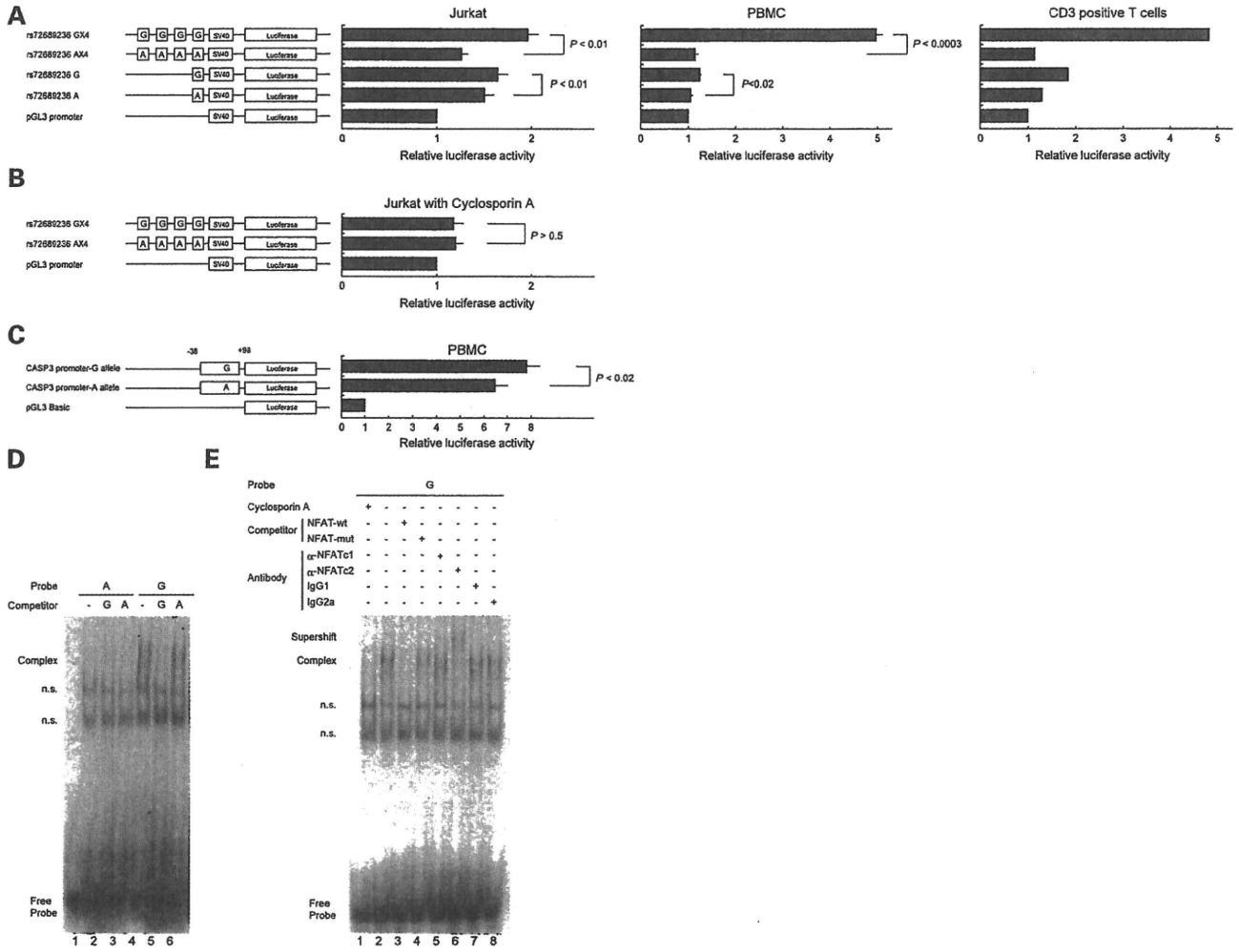

Figure 2. Functional analyses of the G and A alleles of rs72689236. (**A**) Single or four tandem copies of oligonucleotides for the G allele and A allele of rs72689236 were cloned upstream of the SV40 promoter in the PGL3 luciferase reporter vector and transfected into Jurkat cells (left), PBMCs (middle) and $CD3^+$ peripheral T cells (right; single assay). Data represent mean ± SEM of triplicate assays for Jurkat and PBMCs. (**B**) Effect of cyclosporine A on enhancer activity of rs72689236 G allele. (**C**) Transcriptional activity of *CASP3* promoter with different alleles of rs72689236. Data represent mean ± SEM of quintuplicate assays. (**D**) EMSA was performed using nuclear extracts from PBMCs stimulated with ionomycin and PMA. Oligonucleotides corresponding to the A allele (lanes 1–3) and to the G allele (lanes 4–6) were used as probes. Binding reaction was performed with no specific competitor and with excess amounts (×100) of either unlabelled G or A allele oligonucleotides. n.s., non specific bands. (**E**) Binding of NFATs to the rs72689236 G allele was assessed by EMSA using nuclear extracts from PBMCs treated with cyclosporine A in addition to ionomycin and PMA (lane 1), competition assay using oligonucleotides containing an NFAT binding sequence from the human *IL-2* promoter or its mutant (lanes 3 and 4) and a supershift assay with antibodies against NFATc1 (lane 5), NFATc2 (lane 6) and their isotype controls (lanes 7 and 8).

from the *Interleukin-2* (*IL-2*) promoter. And finally the complex was supershifted by a monoclonal antibody against NFATc2 (Fig. 2E).

Allele specific expression of *CASP3*

Next we compared levels of *CASP3* mRNA expressed from different alleles of rs72689236 in PBMCs by allele-specific transcript quantification (ASTQ) experiment. Primers for PCR were designed to encompass a SNP in the 3′-UTR of *CASP3* (rs6948) which was in LD with rs72689236. We examined eight healthy individuals who were heterozygous for both rs72689236 and rs6948, and therefore, inferred to have haplotypes I and III (Fig. 3A). In this haplotype combination, risk allele (A) and non-risk allele (G) of rs72689236 were absolutely linked to C and A allele of rs6948, respectively. The ratio of digested:undigested PCR products was approximately 0.7 for cDNAs and 1.0 for genomic DNA (Fig. 3B, left panel), indicating that the transcript abundance from haplotype III was lower compared with that from haplotype I. Such differences were not observed when the same experiment was conducted on PBMC from five other volunteers who were heterozygous at rs6948 but homozygous for the A allele at rs72689236 (Fig. 3B, right panel). These results suggest an effect of rs72689236 on mRNA expression levels of *CASP3*.

Association study in US KD families of European ancestry

Finally we investigated the association of the 25 variants and KD susceptibility in US subjects of European ancestry. In a

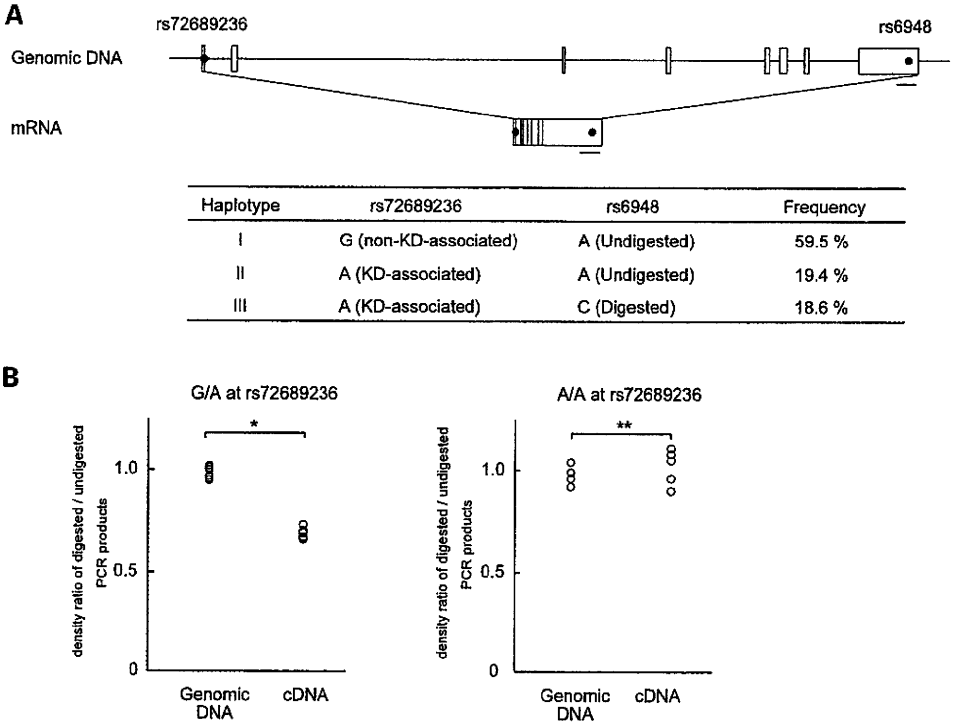

Haplotype	rs72689236	rs6948	Frequency
I	G (non-KD-associated)	A (Undigested)	59.5 %
II	A (KD-associated)	A (Undigested)	19.4 %
III	A (KD-associated)	C (Digested)	18.6 %

Figure 3. Allele-specific transcript quantification (ASTQ) of *CASP3* in PBMC. (**A**) Genomic structure of *CASP3* gene and location of the two SNPs (rs72689236 and rs6948). An amplicon of PCR was indicated by a horizontal bar. Haplotypes for the two SNPs with frequencies larger than 2.5% in the Japanese population were shown. (**B**) Comparison of relative expression level of *CASP3* mRNA from different haplotypes. Ratio of digested and undigested PCR products from genomic DNA and cDNA of PBMCs stimulated with PMA and ionomycin from healthy volunteers heterozygous (left panel; $n = 8$) and homozygous (right panel; $n = 5$) at rs72689236. *two-tailed $P = 3.0 \times 10^{-7}$, **two-tailed $P = 0.40$ by Student's *t*-test.

transmission disequilibrium test performed with US trios, the A allele of rs72689236 was significantly overtransmitted ($n = 249$, OR = 1.54, 95% CI 1.16–2.05, $P = 3.7 \times 10^{-3}$; Table 2). The association of the SNP was no more significant in the subgroup of patients who developed CALs or poorly responded to IVIG therapy in either the Japanese or US populations, indicating that the SNPs influence susceptibility but not disease outcome (data not shown). From both the association study and our functional analyses, we conclude that *CASP3* is a susceptibility gene for KD in Japanese and European American children.

DISCUSSION

KD is an immune-mediated vasculitis that is thought to result from an unknown infectious trigger in genetically susceptible hosts. Our previous findings that downregulation of ITPKC, which functions as a negative regulator of the Ca^{2+}/NFAT pathway in T cells, by an intronic SNP resulted in enhanced activation of the pathway highlighted the importance of regulation of T cell activation in the pathogenesis of KD (5). Caspase-3 is one of the effecter caspases that plays a central role in apoptosis. Peripheral T cells from caspase-3 deficient mice were less susceptible to AICD, a mechanism regulating the magnitude and duration of the T cell immune response (8). Furthermore, it was reported that *Casp3* transcription was selectively up-regulated after T cell receptor (TCR) ligation (12). NFATs are activated by a signal from the TCR and drive transcription of *IL-2* and other cytokines. It was also reported that the induction of *Casp3* mRNA in response to ionomycin stimulation was abolished in Th1 cells from Nfatc2 deficient mice, indicating that NFATc2 is a key transactivator for the gene in this cell type (10). Our data suggest that the sequence surrounding rs72689236 might be a binding site for NFATc2 and acts as an enhancer element in T cells activated in response to signals from TCR. Sequence comparison with chimpanzee indicates that the ancestral allele of rs72689236 is 'G' (data not shown). Interestingly, the GGAA sequence was seen in a similar position within the first non-coding exon of rodent *Casp3* genes (Supplementary Material, Fig. S4), suggesting that the enhancer element might be evolutionarily conserved. There remains a possibility that rs2720378 as well as the other associated variations also affect *CASP3* expression by other, unknown mechanisms. In addition, expression of caspase-3 is not restricted to T cells and a number of proteins are known as substrates for caspases (13). Caspase-3 is also known to play roles in cellular activities other than apoptosis (14–17). Further investigation is needed to understand the impact of reduced *CASP3* expression on the pathogenesis of KD.

We recognize some potential limitations to our study. It is possible that the observed association of the functional polymorphism in *CASP3* with KD susceptibility was somewhat inflated due to population structure. However, the positive linkage signal near *CASP3* in our previous sibpair study and the positive association in our present family-based one, neither of which are influenced by population stratification, suggest that the association has not been over-estimated.

Table 2. Transmission of genetic variants in *CASP3* from European American parents to their offspring with Kawasaki disease

Variants	TDT Risk allele	RAF[a]	T:U[b]	OR	95% CI	*P*-value
rs13108061	–	0.44	114:114	1.00	0.77–1.30	1.00
rs2720382	T	0.83	78:54	1.44	1.02–2.04	0.037
rs2705883	C	0.69	120:80	1.50	1.13–1.99	4.7×10^{-3}
rs4862399	T	0.88	50:49	1.02	0.69–1.51	0.92
rs34605630	C	0.68	122:85	1.44	1.09–1.89	0.010
rs4861629	C	0.81	82:58	1.41	1.01–1.98	0.043
rs7699420	A	0.82	82:63	1.30	0.94–1.81	0.11
rs2705881	C	0.82	82:59	1.39	0.99–1.94	0.053
rs7693625	T	0.81	78:70	1.11	0.81–1.54	0.51
rs1405937	C	0.81	82:62	1.62	0.95–1.84	0.096
rs12108497	G	0.68	122:84	1.45	1.10–1.92	8.1×10^{-3}
Intergene_1	C	0.82	74:58	1.28	0.90–1.80	0.16
Intergene_2	C	0.72	112:78	1.44	1.08–1.92	0.014
rs72689236	A	0.70	120:79	1.54	1.16–2.05	3.7×10^{-3}
rs62339863	T	0.71	122:78	1.56	1.18–2.08	1.9×10^{-3}
casp3_4	G	0.66	134:95	1.41	1.08–1.83	0.010
rs2720379	C	0.68	121:82	1.48	1.11–1.95	6.2×10^{-3}
rs2720378	G	0.68	118:84	1.40	1.06–1.86	0.017
rs4647610	G	0.85	72:53	1.36	0.95–1.94	0.089
rs4647616	G	0.84	70:53	1.32	0.92–1.89	0.13
rs4647617	G	0.84	70:53	1.32	0.92–1.89	0.13
rs59760601	C	0.84	68:49	1.39	0.96–2.00	0.079
rs2720377	A	0.68	121:81	1.49	1.13–1.98	4.9×10^{-3}
rs4647652	C	0.87	58:50	1.16	0.79–1.69	0.44
rs4647655	del (TTCAG GATTT)	0.87	59:50	1.18	0.81–1.72	0.39

[a]Risk allele frequency.
[b]'T' and 'U' indicate transmitted and untransmitted risk alleles of each variant.

Puga *et al.* (18) described that caspase-3 induced by Nfatc2 leads to T cell anergy by downregulating TCR signaling. The transient T cell anergy in KD patients in acute and convalescent phases which have been documented in several reports (19–21) might be, at least partly, related to induction of caspase-3 in T cells by activated NFATc2. No apparent gene–gene interaction between *ITPKC* and *CASP3* was detected in the logistic regression analysis of the SNPs (rs28493229 in *ITPKC* and rs2720378 or rs72689236 in this study, data not shown). However, it is of great interest that NFAT is involved in both pathways in which these SNPs have a functional role (Supplementary Material, Fig. S5). It has also been reported that Nfatc2 is a substrate for caspase-3 (22). It may be that the induction of caspase-3 acts as a negative feedback mechanism to regulate activation of the Ca^{2+}/NFAT pathway. There are likely to be several molecular networks playing major roles in the pathogenesis of KD. Our present findings further highlight the Ca^{2+}/NFAT pathway as a main axis in regulating these networks. Since many inhibitors of this pathway such as cyclosporine and tacrolimus are in clinical use, further elucidation of the role of caspase-3 in the pathophysiology of KD may lead to new preventive and therapeutic strategies for this vasculitis.

MATERIALS AND METHODS

DNA samples

We recruited 920 Japanese KD patients from several medical institutes in Japan. All Japanese KD patients (male:female:no info = 554:365:1) were diagnosed by pediatricians according to the Japanese criteria (23). Median age of disease onset was 23.0 months (range 1–136). Healthy Japanese adults without a history of KD ($n = 1409$) were also recruited as controls from several medical institutes. DNA samples from 249 KD subjects of European descent (male:female = 163:86) and their biological parents were collected by several medical institutes participating in the US KD Genetics Consortium. The study was approved by the ethical committee of RIKEN and the institutional review board of all participating institutions. Written informed consent and assent as appropriate were obtained from subjects and their parents.

Re-sequencing and genotyping

Data regarding tagging SNPs were obtained from the website of International HapMap Project (http://hapmap.ncbi.nlm.nih.gov/cgi-perl/gbrowse/hapmap24_B36/). LD map in Figure 1 was created using Haploview 4.1 software (http://www.broad.mit.edu/haploview/haploview). For SNP discovery, we resequenced the genomic region (NT_022792.17: from nt 17,956,305 to 17,992,719) using DNA from 12 KD patients and 12 controls. Repetitive sequences except for those in the region from the promoter to intron 1 of *CASP3* were excluded from the analysis. We genotyped SNPs and insertion/deletion polymorphisms using the Invader assay (24) and direct sequencing, respectively.

Statistic analysis

Association of the SNPs was analyzed using a chi-square test. Meta-analysis of data from case–control sets was conducted by Mantel–Haenszel methodology. Transmission disequilibrium test was performed using TDT software (25) integrated in Haploview 4.1. Haplotype analysis was conducted by using the program THESIAS (26) (http://genecanvas.ecgene.net/news.php) and conditional log-likelihood with Akaike information criterion (AIC): AIC = $-2 \times$ (the maximized value of the conditional log-likelihood) $+ 2 \times$ (the number of parameters). As the number of parameters, we used the number of alleles or haplotypes with frequencies >0.01 that were used for each model. In the logistic regression analysis of a SNP, we first applied a 1 degree-of-freedom (1 d.f.) likelihood ratio test to determine whether a 1 d.f. multiplicative allelic effects model or a 2 d.f. full genotype model was more appropriate (26). Because we did not find any significant difference from the full genotype model ($P > 0.05$), we assumed a multiplicative allelic effects mode. Next, we carried out a forward logistic regression analysis, where we started by assessing whether the most significant SNP was sufficient to model the association among the SNP set. For this, we used a 1 d.f. likelihood ratio test for adding each of the remaining SNPs to the model by assuming multiplicative allelic effects for the additional SNPs.

Luciferase assay

Jurkat E6-1 cells and HeLa cells were obtained from ATCC and the RIKEN Cell Bank, respectively. PBMCs from healthy volunteers were separated from venous blood using

Lymphoprep reagent (Axis-Shields). $CD3^+$ T cells were isolated using iMag system with a monoclonal antibody against human CD3 (clone HIT3a) conjugated with magnetic beads (BD Biosciences). We cloned single or four tandem copies of 31 nucleotides for each SNP region upstream of the SV40 promoter of the pGL3-promoter vector (Promega). The minimal promoter region of *CASP3* (nt −38 of 5′ flanking to +17 of intron 1) was cloned into pGL3-basic vector. These reporter plasmids were co-transfected with phRGTK vector into the cells. C-016 and O-005 programs of the Nucleofector (Amaxa) were used for transfection into Jurkat E6-1 and HeLa, respectively. Transfection into PBMCs and $CD3^+$ T cells was conducted with U-014 program. Twenty-four hours after transfection, Jurkat cells, PBMCs and $CD3^+$ T cells were stimulated with 1 μg/ml of ionomycin (SIGMA) and 50 ng/ml of PMA (SIGMA) for 4 h and harvested. Suppression of NFAT activity was performed by adding 100 ng/ml of cyclosporin A (CALBIOCHEM) in the above-mentioned stimulation medium. Luciferase activity was measured with the Dual Luciferase Reporter Assay system (Promega). We also cloned cDNAs of NFATc1 (NM_172390) and NFATc2 (NM_173091) into pcDNA3.1(+) (Invitrogen) and co-transfected with reporter vectors for rs72689236 to test the effect of overexpression of these proteins on enhancer activity.

Electorophoretic mobility shift assay

PBMCs were incubated in RPMI 1640 medium supplemented with 10% of fetal bovine serum and stimulated with ionomycin (1 μg/ml) and PMA (50 ng/ml) for 2 h. Suppression of NFAT activity was achieved by adding 100 ng/ml of cyclosporin A to the stimulation medium. After lysing the cells with buffer A [10 mM HEPES-KOH (pH 7.8), 10 mM KCl, 0.1 mM EDTA, 0.1% NP-40 and protease inhibitor cocktail], nuclear extracts were prepared using buffer C [50 mM HEPES-KOH (pH 7.8), 420 mM KCl, 0.1 mM EDTA, 5 mM $MgCl_2$, 2% glycerol and protease inhibitor cocktail]. Eighteen base pairs of double-stranded oligonucleotides corresponding to G and A alleles of rs72689236 were labeled with digoxygenin -11-ddUTP using DIG Gel Shift Kit (Roche). Probes were incubated with 5 μg of nuclear extract pre-incubated with 0.2 μg of poly d(I-C), 1 μg of poly-L-lysin for 30 min in room temperature. For the supershift assay, nuclear extract and monoclonal antibodies (Santa Cruz) or isotype control IgGs (R&D SYSTEMS) were incubated for 1 h on ice prior to the binding reaction. Competition was conducted with 100× molar excess of unlabeled oligonucleotides. Sequences of the oligonucleotides are provided in Supplementary Material, Table S4. The binding reaction mixtures were separated on 5% non-denaturing polyacrylamide gel in 0.5 × TBE buffer, transferred onto a nylon membrane and detected with a chemiluminescent system (Roche).

Allele-specific transcript quantification

ASTQ was carried out as described previously (27). Sequences of primers for PCR were shown in Supplementary Material, Table S5. Total RNA was extracted from PBMCs after stimulation for 4 h with 1 μg/ml of ionomycin and 50 ng/ml of PMA. Genomic DNAs and cDNAs were amplified for 36 cycles with the primers. At the last cycle, reverse primer labeled with Alexa Fluor 488 at the 5′ was added. Amplicons were digested with *Ban*II (Takara) according to manufacturer's instruction. Separation was conducted on 12% non-denaturing polyacrylamide gels in 25 mM Tris and 250 mM glycine. Visualization and quantification of digested and undigested PCR products was carried out by using FLA-7000 analyzer and Multiguage software (Fujifilm).

Accession codes

Genbank: human chromosome 4 genomic DNA sequence, NT_022792.17; mRNA sequences for human *CASP3*, NM_004346.3 and NM_032991.2.

SUPPLEMENTARY MATERIAL

Supplementary Material is available at *HMG* online.

ACKNOWLEDGEMENTS

We thank the KD patients and their families as well as all the medical staff taking care of the patients. We are grateful to Tomoyo Matsubara, Makoto Nishibatake, Hiroyuki Aotsuka, Hiromichi Nakajima, Fumiyo Kudo, Ryota Ebata, Tetsuya Sano, Toru Matsushita, Kyoko Suzuki, Kunihiro Akagi, Takeshi Isobe, Satoko Ogita, Shozo Oku, Takeo Tanaka, Yuji Tanaka, Yuichi Nomura, Masako Sakauchi, Hideo Cho, Akiyoshi Nariai, Masaru Miura, Masao Nakagawa, Youichi Kaburagi and other pediatricians who contributed Japanese DNA samples. We appreciate Tomohiko Gunji for fruitful discussion. We thank Joan Pancheri, MSN and Nancy Innocentini RN for collection of DNA samples and DeeAnna Scherrer, Hiroko Sugiyama, Masako Saito, Saori Kawakami and Yoshie Kikuchi for technical assistance.

Conflict of Interest statement. None declared.

FUNDING

This work was supported by grants from the Millennium Project, from Japan Kawasaki disease Research Center and from the Ministry of Health, Labour and Welfare (0401040 to A.H.) and by a grant from the Heart, Lung and Blood Institute of the National Institutes of Health (HL-06941 to J.C.B.).

REFERENCES

1. Kawasaki, T. (1967) Acute febrile mucocutaneous syndrome with lymphoid involvement with specific desquamation of the fingers and toes in children. *Arerugi*, **16**, 178–222.
2. Burns, J.C. (2002) Commentary: translation of Dr. Tomisaku Kawasaki's original report of fifty patients in 1967. *Pediatr. Infect. Dis. J.*, **21**, 993–995.
3. Kato, H., Koike, S., Yamamoto, M., Ito, Y. and Yano, E. (1975) Coronary aneurysms in infants and young children with acute febrile mucocutaneous lymph node syndrome. *J. Pediatr.*, **86**, 892–898.
4. Onouchi, Y., Tamari, M., Takahashi, A., Tsunoda, T., Yashiro, M., Nakamura, Y., Yanagawa, H., Wakui, K., Fukushima, Y., Kawasaki, T.

et al. (2007) A genomewide linkage analysis of Kawasaki disease: evidence for linkage to chromosome 12. *J. Hum. Genet.*, **52**, 179–190.
5. Onouchi, Y., Gunji, T., Burns, J.C., Shimizu, C., Newburger, J.W., Yashiro, M., Nakamura, Y., Yanagawa, H., Wakui, K., Fukushima, Y. *et al.* (2008) ITPKC functional polymorphism associated with Kawasaki disease susceptibility and formation of coronary artery aneurysms. *Nat. Genet.*, **40**, 35–42.
6. Yi, Q.J., Li, C.R. and Yang, X.Q. (2001) Effect of intravenous immunoglobulin on inhibiting peripheral blood lymphocyte apoptosis in acute Kawasaki disease. *Acta Paediatr.*, **90**, 623–627.
7. Tsujimoto, H., Takeshita, S., Nakatani, K., Kawamura, Y., Tokutomi, T. and Sekine, I. (2001) Delayed apoptosis of circulating neutrophils in Kawasaki disease. *Clin. Exp. Immunol.*, **126**, 355–364.
8. Woo, M., Hakem, R., Soengas, M.S., Duncan, G.S., Shahinian, A., Kägi, D., Hakem, A., McCurrach, M., Khoo, W., Kaufman, S.A. *et al.* (1998) Essential contribution of caspase 3/CPP32 to apoptosis and its associated nuclear changes. *Genes Dev.*, **12**, 806–819.
9. Hirota, J., Furuichi, T. and Mikoshiba, K. (1999) Inositol 1,4,5-trisphosphate receptor type 1 is a substrate for caspase-3 and is cleaved during apoptosis in a caspase-3-dependent manner. *J. Biol. Chem.*, **274**, 34433–34437.
10. Macián, F., García-Cózar, F., Im, S.H., Horton, H.F., Byrne, M.C. and Rao, A. (2002) Transcriptional mechanisms underlying lymphocyte tolerance. *Cell*, **109**, 719–731.
11. Northrop, J.P., Ho, S.N., Chen, L., Thomas, D.J., Timmerman, L.A., Nolan, G.P., Admon, A. and Crabtree, G.R. (1994) NF-AT components define a family of transcription factors targeted in T-cell activation. *Nature*, **369**, 497–502.
12. Sabbagh, L., Bourbonnière, M., Sékaly, R.P. and Cohen, L.Y. (2005) Selective up-regulation of caspase-3 gene expression following TCR engagement. *Mol. Immunol.*, **42**, 1345–1354.
13. Fischer, U., Jänicke, R.U. and Schulze-Osthoff, K. (2003) Many cuts to ruin: a comprehensive update of caspase substrates. *Cell Death Differ.*, **10**, 76–100.
14. Woo, M., Hakem, R., Furlonger, C., Hakem, A., Duncan, G.S., Sasaki, T., Bouchard, D., Lu, L., Wu, G.E., Paige, C.J. *et al.* (2003) Caspase-3 regulates cell cycle in B cells: a consequence of substrate specificity. *Nat. Immunol.*, **4**, 1016–1022.
15. Alam, A., Cohen, L.Y., Aouad, S. and Sékaly, R.P. (1999) Early activation of caspases during T lymphocyte stimulation results in selective substrate cleavage in nonapoptotic cells. *J. Exp. Med.*, **190**, 1879–1890.
16. Kennedy, N.J., Kataoka, T., Tschopp, J. and Budd, R.C. (1999) Caspase activation is required for T cell proliferation. *J. Exp. Med.*, **190**, 1891–1896.
17. Miossec, C., Dutilleul, V., Fassy, F. and Diu-Hercend, A. (1997) Evidence for CPP32 activation in the absence of apoptosis during T lymphocyte stimulation. *J. Biol. Chem.*, **272**, 13459–13462.
18. Puga, I., Rao, A. and Macián, F. (2008) Targeted cleavage of signaling proteins by caspase 3 inhibits T cell receptor signaling in anergic T cells. *Immunity*, **29**, 193–204.
19. Masuda, K., Takei, S., Nomura, Y., Imanaka, H., Sameshima, K. and Yoshinaga, M. (1998) Transient low T cell response to streptococcal pyrogenic exotoxin-C in patients with Kawasaki disease. *Pediatr. Res.*, **44**, 27–31.
20. Kollmann, T.R., Klein, E.J., Stefanelli, C.B. and Marcuse, E.K. (2001) Purified protein derivative anergy in Kawasaki disease. *Pediatr. Infect. Dis. J.*, **20**, 81–82.
21. Kuijpers, T.W., Wiegman, A., van Lier, R.A., Roos, M.T., Wertheim-van Dillen, P.M., Pinedo, S. and Ottenkamp, J. (1999) Kawasaki disease: a maturational defect in immune responsiveness. *J. Infect. Dis.*, **180**, 1869–1877.
22. Wu, W., Misra, R.S., Russell, J.Q., Flavell, R.A., Rincón, M. and Budd, R.C. (2006) Proteolytic regulation of nuclear factor of activated T (NFAT) c2 cells and NFAT activity by caspase-3. *J. Biol. Chem.*, **281**, 10682–10690.
23. Ayusawa, M., Sonobe, T., Uemura, S., Ogawa, S., Nakamura, Y., Kiyosawa, N., Ishii, M. and Harada, K. (2005) Revision of diagnostic guidelines for Kawasaki disease (the 5th revised edition). *Pediatr. Int.*, **47**, 232–234.
24. Suzuki, A., Yamada, R., Chang, X., Tokuhiro, S., Sawada, T., Suzuki, M., Nagasaki, M., Nakayama-Hamada, M., Kawaida, R., Ono, M. *et al.* (2003) Functional haplotypes of PADI4, encoding citrullinating enzyme peptidylarginine deiminase 4, are associated with rheumatoid arthritis. *Nat. Genet.*, **34**, 395–402.
25. Spielman, R.S., McGinnis, R.E. and Ewens, W.J. (1993) Transmission test for linkage disequilibrium: the insulin gene region and insulin-dependent diabetes mellitus (IDDM). *Am. J. Hum. Genet.*, **52**, 506–516.
26. Tregouet, D.A. and Garelle, V. (2007) A new JAVA interface implementation of THESIAS: testing haplotype effects in association studies. *Bioinformatics*, **23**, 1038–1039.
27. Uejima, H., Lee, M.P., Cui, H. and Feinberg, A.P. (2000) Hot-stop PCR: a simple and general assay for linear quantitation of allele ratios. *Nat. Genet.*, **25**, 375–376.

Journal of Human Genetics (2010), 1–8

www.nature.com/jhg

ORIGINAL ARTICLE

Replication of genetic association studies in asthma and related phenotypes

Siizkhuu Undarmaa[1], Yoichi Mashimo[1], Satoshi Hattori[1], Naoki Shimojo[2], Kimie Fujita[3], Akihiko Miyatake[4], Satoru Doi[5], Yoichi Kohno[2], Yoshitaka Okamoto[6], Tomomitsu Hirota[7], Mayumi Tamari[7], Akira Hata[1] and Yoichi Suzuki[1]

In asthma genetics, the association of highly replicated susceptibility genes lacks consistency across populations. To identify genuine associations, we investigated the reproducibility of the 23 most promising asthma and asthma-related candidate genes in a moderately sized sample from the Japanese population. We compared the frequency of 33 polymorphisms in unrelated cases and controls and tested for their association with asthma, atopy and serum total IgE levels using allele frequency, codominant, dominant and recessive genotype models. On the basis of the consistency of our findings with previous meta-analyses and large replication studies, *IL13*, *TNF*, *ADAM33*, *IL4RA* and *TBXA2R* might represent common major asthma and asthma-related trait genes. Individual gene assessment was extended to the interactions between two polymorphisms using our original method. Interactions between *TBXA2R* and *ADAM33*, and *IL4RA* and *C3* were suggested to increase the risk for childhood and all asthma (adult and childhood asthma combined). The confirmation of previously reported associations between gene polymorphisms and phenotypes was problematic when as few as several hundred samples per group were used. Stratification of the subjects by environmental factors or other confounding factors may be necessary to improve the sensitivity and reliability of association results.
Journal of Human Genetics advance online publication, 16 April 2010; doi:10.1038/jhg.2010.32

Keywords: association; asthma; atopy; polymorphism; replication

INTRODUCTION

Asthma is a heritable trait[1] and investigations to determine the genetic components underlying asthma using linkage mapping and the candidate gene approach have been carried out. By 2006, more than 100 genes were associated with asthma and asthma-related phenotypes;[2] 25 of these genes have been replicated in more than six independent association studies. In 2008, this list was complemented with an additional three genes, *FLG*, *NAT2* and *CCL15*.[3] However, no single polymorphic marker or gene locus has been unanimously labeled as a strong and independent genetic determinant of asthma, and the results for the highly replicated genes have been inconsistent across the tested populations.[3]

To identify true associations, it is of critical importance to comprehensively replicate the initial finding.[4] To this aim, we investigated whether the 23 most replicated genes for asthma and asthma-related phenotypes were positively associated with extrinsic childhood and adult asthma, atopy and total serum IgE levels in a moderately sized sample drawn from the Japanese population.

We also tested eight genes that were significantly associated with asthma in our subjects: *IL13*,[5] *TBXA2R*,[6] *GSTP1*,[7] *ADAM33*,[8] *MMP9*,[9] *IL12B*,[10] *C3*[11] and *SOCS1*.[12] The re-evaluation of these associations is conditioned by the limitations of the original reports in which childhood asthma included subjects with nonatopic asthma and those who were <4 years of age. The adult asthma cases also included nonatopic asthma in some of these reports. Moreover, the comparison of the childhood asthma group was with an adults-only control group. In this study, we redefined the atopic asthma patients, introduced age-matched child controls and re-evaluated the association of these genes with the asthma phenotypes, atopy and total serum IgE levels.

Further, we extended the assessment of individual genes to identify potential interactions between the genes, as increasing knowledge about biological pathways and gene networks implies that gene–gene interactions are important and must be taken into account when estimating the genetic risk of a disease.[13]

MATERIALS AND METHODS

Study population

The asthma population was restricted to extrinsic asthma patients with subsequent distinction between childhood and adult asthma by cutoff age of below or above 16 years old regardless of the age of the disease onset. We recruited 325 subjects with childhood atopic asthma, 367 adults with atopic

[1]Department of Public Health, Graduate School of Medicine, Chiba University, Chiba, Japan; [2]Department of Pediatrics, Graduate School of Medicine, Chiba University, Chiba, Japan; [3]School of Human Nursing, The University of Shiga Prefecture, Shiga, Japan; [4]Miyatake Asthma Clinic, Osaka, Japan; [5]Department of Pediatric Allergy, Osaka Prefectural Medical Center for Respiratory and Allergic Diseases, Osaka, Japan; [6]Department of Otolaryngology, Graduate School of Medicine, Chiba University, Chiba, Japan and [7]Laboratory for Respiratory Diseases, Center for Genomic Medicine, RIKEN, Kanagawa, Japan
Correspondence: Dr Y Suzuki, Department of Public Health, Chiba University Graduate School of Medicine, 1-8-1 Inohana, Chuo-ku, Chiba 260-8670, Japan.
E-mail: ysuzuki@faculty.chiba-u.jp
Received 30 November 2009; revised 15 March 2010; accepted 24 March 2010

asthma and 646 adult controls from Osaka City, Japan. The details of these subjects have been described elsewhere.[10,12,14] For childhood controls and the investigation of total and specific IgE levels, we recruited children attending an elementary school in Chiba City, Japan. The clinical characteristics of this population as well as inclusion and exclusion criteria have been described previously.[15] In brief, after the exclusion of questionnaire-assessed asthma and/or atopic dermatitis subjects and those with congenital heart diseases and lung diseases caused by premature birth, 336 children having a complete set of information on the total and eight specific IgE levels, genotypes and environmental factors were assigned to the child control group. The mean ages (range) of the four groups were as follows: childhood asthma, 9.9 (4–15); adult asthma, 45 (16–83); child controls, 9.3 (6–12); and adult control, 43.7 (20–75) years. Written informed consent was received from all participants and the study was approved by the ethics committees of Chiba University Graduate School of Medicine and RIKEN.

Gene and polymorphism selection

The list of candidate gene polymorphisms included in this study, their location within the gene and corresponding rs numbers are given in Supplementary Table S1. In this table, we also included the allele frequency in child and adult control populations.

The most replicated genes were selected based on the list created by Ober and Hoffjan.[2] From the 25 cited genes, we intentionally excluded *HLA-DRB1* and *HLA-DBP1* from our analysis due to the high number of variants linked to asthma and asthma-related phenotypes, the genotyping of which would surpass our capacity. The remaining 23 genes were tested for association based on the most positively reported polymorphisms and are represented by Group 1 (>10) and Group 2 (6–10), depending on the number of their replications (Supplementary Table S1). We included four genes (*MMP9, IL12B, C3* and *SOCS1*), which were not in the original 23 genes, but were found to be associated with asthma in our previous studies (Supplementary Table S1, Group 3). These were tested for association with the same positive polymorphisms as in the initial reports.

DNA extraction and genotyping

Genomic DNA was prepared from peripheral blood samples using the standard protocols. Whole genome amplification was carried out using the Illustra GenomiPhi V2 DNA Amplification Kit (GE Healthcare, Buckinghamshire, UK) according to the manufacturer's instructions. Genotyping was carried out by means of allele-specific amplification, single-nucleotide primer extension reaction or fragment analysis of the PCR product. The genotyping methods used for each polymorphism are given in Supplementary Table S1 and the primer sequences are shown in Supplementary Tables S2, S3a, S3b and S4. The results obtained by these molecular assays were analyzed on ABI PRISM 3100 Genetic Analyzer and ABI PRISM 7000 Sequence Detector Systems (Applied Biosystems, Foster City, CA, USA), or by using Chromo4 Real-Times System (Bio-Rad Laboratories, Hercules, CA, USA). The detailed genotypic protocols are described in Supplementary Methods.

Statistical analysis

A case–control study design was used to analyze the associations between gene variants and the dichotomous phenotypes. We calculated allele frequencies and tested their agreement with Hardy–Weinberg equilibrium (HWE) using a χ^2 goodness-of-fit test. We compared differences in the allele frequencies and genotype distribution of each polymorphism between the case and control subjects by using a 2×2 (allele) or 2×3 contingency χ^2-test (dominant, codominant and recessive genotype models) with 1 or 2 degree of freedom. Total serum IgE values were logarithm transformed to approximate a normal distribution and analyzed as a quantitative trait using two different tests: linear regression analysis with age and sex as covariates; and analysis of variance (ANOVA). All statistical analyses were carried out with SPSS Statistics 17.0 (SPSS Japan Corporation, Tokyo, Japan). The statistical power of this study was calculated using SamplePower 2.0 (SPSS Corporation). *P*-values <0.05 were judged to be significant; as there was an *a priori* hypothesis with all tested polymorphisms, we did not adjust the significance levels for multiple testing.

Interactions between two polymorphisms were screened using a program written in Excel VBA (Microsoft Japan, Tokyo, Japan). This program identified every possible pairing of polymorphisms, calculated the χ^2 and *P*-values of contingency tables between the genotype of one polymorphism and the disease after stratification by the genotype of the other polymorphism. The program then calculated the χ^2 and *P*-values for the goodness-of-fit statistics of the distribution pattern of genotype vs disease table with stratification against no stratification. Single-nucleotide polymorphisms (SNPs) in the same gene were not tested for this interaction because most of them showed linkage disequilibrium.

RESULTS

Statistical power of this study

We estimated the frequency difference between the case and control groups, and odds ratio (OR) for our samples with different genotype/allele frequencies according to sample size. We set our detection power at 80% with an α level of 0.05.

Supplementary Table S5a shows the results of this calculation for the asthma cases, when estimation was carried out for given genotype/allele frequencies among their respective control peers. Adult asthma group had slightly better power than the childhood asthma group because of almost twice bigger number of adult controls compared with the child controls. In the case of adult asthma, enough (>80%) power could be expected for polymorphisms with an OR of 1.4 when the minor genotype frequency was from 30–60%. In the allele frequency comparison, there was slightly more detection power than for the genotype comparison, as the number of alleles was twice that of the genotype. When we estimated the genotype/allele frequencies in child asthmatics for given adult control genotype/allele frequencies (Supplementary Table S5b), as expected, some increase in power could be observed with ORs getting closer to those of childhood asthma vs child control estimation. In case of calculation based on the comparison between combined asthma subjects and combined controls (Supplementary Table S5b), ORs of 1.3 and 1.2 could be detected for minor genotype and allele frequencies of 30–60%, respectively.

The estimated power to detect an association between atopy and genetic polymorphisms (Supplementary Table S6) was comparatively inferior to that of asthma with an OR of 1.9.

Association of the 23 genes with childhood and adult atopic asthma

The genotype frequencies of all gene variants, except for *GSTM1* ins/del, were in Hardy–Weinberg equilibrium (goodness-of-fit χ^2-test, $P>0.01$) in adult and child controls. We could not test the *GSTM1* ins/del variant for Hardy–Weinberg equilibrium because the genotyping method did not distinguish between ins/del heterozygotes and homozygotes.

The summary of results for basic comparison between cases and controls is presented in Table 1, in which only polymorphisms with *P*-value <0.05 in at least one genetic model test are shown. When the frequency of polymorphisms in childhood asthmatics were compared with those of asthma free children, the most strong candidate variant was *IL13* −1112C>T, which was significantly associated in all but dominant genotype model; *LTC4S* was positively associated in the allele frequency and dominant model tests and *CCL5* −28C>G resulted in significant difference only in the dominant genotype model. In the adult samples, there were significant differences noted between the controls and the asthma patients for *TNF, ADAM33* and *NOS1*. *TNF* showed positive results in the allele frequency, codominant and dominant models. Association of *ADAM33* Met764Thr variant with adult asthma was significant for allele frequency and dominant genotype models. There was strong association of both *NOS1* variants with the disease in all tests except for GT repeat intron

Table 1 Association of genotyped polymorphisms with the asthma phenotypes (basic comparisons)

		Case–control study P-value											
		Childhood asthma vs child control				*Adult asthma vs adult control*				*All asthma vs all controls*			
Gene	*Polymorphism*	*Allele*	*Codom.*	*Dom.*	*Rec.*	*Allele*	*Codom.*	*Dom.*	*Rec.*	*Allele*	*Codom.*	*Dom.*	*Rec.*
Group 1													
IL13	Arg110Gln	×	×	×	×	×	×	×	×	×	×	×	×
	−1112C>T	0.014	0.011	×	0.003	×	×	×	×	×	×	×	×
TNF	−1037C>T	×	×	×	×	0.001	0.003	0.001	×	0.003	0.014	0.005	×
ADAM33	Met764Thr	×	×	×	×	0.008	×	0.005	×	0.029	×	0.035	×
	13236C>T	×	×	×	×	×	×	×	×	0.038	×	×	×
Group 2													
LTC4S	−444A>C	0.023	×	0.026	×	×	×	×	×	×	×	×	×
NOS1	GT repeat intron 2 (187 allele)	×	×	×	×	0.0003	0.002	0.001	0.011	0.026	×	×	×
	GT repeat intron 2 (183 allele)	×	×	×	×	0.007	0.022	0.007	×	0.045	×	×	×
CCL5	−403A>G	×	×	×	×	×	×	×	×	×	×	×	×
	−28C>G	×	×	0.048	×	×	×	×	×	×	×	×	×
Group 3													×
MMP9	2127G>T	×	×	×	×	×	×	×	×	×	×	×	×
	5546G>A	×	×	×	×	×	×	×	×	×	×	×	×
IL12B	−6415CTCTAA>GC	0.010	0.006	×	0.001	×	×	×	×	0.012	0.009	×	0.002
	1146 C> A	0.019	0.010	×	0.003	×	×	×	×	0.003	0.003	×	0.001
C3	Block 2 (haplotype 6)[a]	0.017	×	×	×	×	×	×	×	0.015	0.022	0.010	×
	Block 4 (haplotype 1)[a]	×	×	×	×	0.001	0.002	0.024	0.002	0.001	0.005	0.003	0.019
SOCS1	−1478CA>del	×	×	×	×	0.0005	0.002	0.002	0.015	0.002	0.005	0.006	0.017

Abbreviations: Allele, χ^2-test of allele frequency; codom., 2×3 codominant model genotype χ^2-test; dom., 2×2 dominant model genotype χ^2-test; rec., 2×2 recessive model genotype χ^2-test.
[a]For haplotype description please refer Inoue *et al.*[11]
Polymorphisms with a *P*-value ⩾0.05 in all association tests of the four genetic models are not shown.
×$P \geqslant 0.05$.

(183 allele) in the recessive genotype model. In the association test between the polymorphisms and all asthma, that is child and adult asthma combined, significant associations were observed for the same genes as in adult asthma. *TNF* and *ADAM33* Met764Thr remained positively associated with asthma in the allele frequency, codominant and dominant models alike in the single adult asthma group comparison. The association of *NOS1* variants became weaker with significance only in allele frequency model. Additional significant association was observed only for *ADAM33* 13236C>T in the allele frequency model.

Conditioned by the inherent characteristics of our case and control samples, we extended our analysis further (Table 2). In our child control group, we recognize the potential presence of asthma susceptibility gene variants carriers who might become asthmatics later in life, and consequently, to become a source of bias. Addressing this issue, we tested childhood asthmatics also with adult controls, considering the later ones as more reliable asthma 'free' subjects. Paradoxically, the previous significant associations found in the comparison for child asthma vs child control disappeared; instead, *TNF, IL4RA, ADAM33, GSTM1, AAA1* and *NOS1* showed significant results. The substantial difference in results between childhood asthma vs child control and childhood asthma vs adult control tests might be due to some confounding effects of hidden genetic and environmental heterogeneities between child and adult control groups.

Furthermore, as the natural history of asthma in some adults starts during childhood, we characterized the association results after stratifying adult asthma cases by age at the onset (Table 2). Using the same cutoff age (<16 years) as for discerning childhood asthma from adult asthma, we obtained 118 adults (32% of adult asthma), who have reported physician diagnosed asthma during their childhood, and 249 adults with newly onset bronchial asthma. To elucidate the genes associated with differential onset of asthma in children, we merged the child-onset adult subgroup with childhood asthma group (all L16 adult atopic asthma (BA)) and tested with either child or adult controls by applying the same strategy as used in the nonstratified adult asthma. In the association test with child control, besides the previously detected gene variants in the comparison of child asthma vs child control, *TNF* showed at least one significant association in four association tests, whereas the significance of *CCL5* disappeared. When the combined child-onset asthma group was compared with adult controls, the observed associations in child asthma vs adult control comparison could be confirmed for only *IL4RA* Ile50Val and *ADAM33* 13236C>T polymorphisms. We next examined the new-onset adult asthma, in which *TNF* and *ADAM33* Met764Thr have retained their significant associations found with the onset nonstratified adult asthma. In addition, *IL13, IL4RA* and *GSTM1* have emerged as genes associated with asthma establishment during adulthood. Interestingly, the two *ADAM33* polymorphisms were associated with different asthma phenotypes when comparisons were carried out with adult control. *ADAM33* Met764Thr was significantly associated with adult asthma, whereas *ADAM33* 13236C>T variant was significantly more frequent in childhood asthma and all child-onset asthma groups.

We also compared the distribution of polymorphisms between the two control groups; it showed a relative homogeneity with significant

Table 2 Summary of the association results between polymorphisms and asthma when case and control groups were compared in various combinations

		Two group comparison							
Gene	*Polymorphism*	*Child BA vs child CO*	*Child BA vs adult CO*	*Adult BA vs adult CO*	*All L16 BA vs child CO*	*All L16 BA vs adult CO*	*M16 adult BA vs adult CO*	*Child CO vs adult CO*	*Child BA vs adult BA*
Group 1									
IL13	Arg110Gln	×	×	×	×	×	×	×	×
	−1112C>T	°	×	×	°	×	°	°	×
TNF	−1037C>T	×	°	°	°	×	°	×	×
IL4RA	Ile50Val	×	°	×	×	°	°	×	×
	Gln551Arg	×	×	×	×	×	×	×	°
ADAM33	Met764Thr	×	×	°	×	×	°	×	°
	13236C>T	×	°	×	×	°	×	×	°
Group 2									
GSTM1	Ins/del	×	°	×	×	×	°	×	°
IL10	571C>A	×	×	×	×	×	×	×	°
LTC4S	−444A>C	°	×	×	°	×	×	°	×
AAA1	522363G>C	×	°	×	×	×	×	×	°
NOS1	GT repeat (187 allele)	×	°	°	×	×	×	×	°
	GT repeat (183 allele)	×	×	°	×	×	×	×	×
CCL5	−28C>G	°	×	×	×	×	×	×	×
Group 3									
MMP9	2127G>T	×	°	×	×	×	°	°	×
	5546G>A	×	°	×	×	°	×	°	×
IL12B	−6415ins/del	°	°	×	°	°	×	×	°
	1146 C> A	°	°	×	°	°	×	×	°
C3	Block 2 (haplotype 6)[a]	°	×	×	°	°	×	×	×
	Block 4 (haplotype 1)[a]	×	°	°	×	°	×	×	×
SOCS1	−1478CA>del	×	×	°	×	°	×	×	×

Abbreviations: Child BA, childhood atopic asthma; child CO, child controls; adult BA, adult atopic asthma; adult CO, adult controls; all L16 adult BA, childhood atopic asthma and adult atopic asthma at onset age <16 years combined; M16 adult BA, adult atopic asthma at onset age ⩾16.
[a]For haplotype description please refer Inoue *et al.*[11]
Polymorphisms with a *P*-value ⩾0.05 in all association tests of the four genetic models are not shown.
°*P*-value <0.05 in at least one association test of the four genetic models.
×None of the *P*-value in the four genetic models was <0.05.

difference only for *IL13* and *LTC4S*. It indicates that there would be little bias created using either sample as a control group for any of the case groups and justifies our combining of the two control groups to form a single one in the comparison for all asthma vs all control. In the comparison test for childhood asthma vs adult asthma, *IL4RA*, *ADAM33*, *GSTM1*, *IL10*, *AAA1* and *NOS1* genes were found significantly different, which is coherent with the case–control comparison results.

Association of the 23 genes with atopy

ADAM33 13236C>T, *NOS1* GT repeat 183 bp allele and *TBXA2R* 795T>C were significantly associated with atopy in the recessive or dominant models (Supplementary Table S7). *NOS1* and *TBXA2R* also showed significant association in the allele frequency test, whereas *ADAM33* did not.

Association of the 23 genes with total serum IgE

Supplementary Table S8 summarizes the relationship between the mean of $\log_{10}$-transformed total serum IgE level and gene variants. There was a significant association between *GSTP1* and total IgE level as determined by ANOVA that remained significant after adjusting for age and gender as covariates in linear regression analysis.

Re-evaluation of the associations previously discovered in our subjects

We confirmed the association of the *IL13*, *ADAM33*, *MMP9*, *IL12B*, *C3* and *SOCS1* polymorphisms with atopic asthma (Tables 1 and 2). The association of *TBXA2R* with asthma was not replicated; instead, we identified an association of *TBXA2R* with atopy (Supplementary Table S7). Comparatively to our previous studies, in this study we also investigated the polymorphisms for association with serum IgE level. Significant results were observed for *GSTP1* as described above and for *MMP9* 5546G>A (Supplementary Table S8).

Screening of gene–gene interactions

From the 40 genetic polymorphisms, polymorphism pairs with a *P*-value for association with the disease of <0.05 and a *P*-value for interaction <0.01 are listed in Table 3. A pair of *LTA* and *TNF* SNPs showed a very small *P*-value; however, these two genes are physically close and these SNPs are known to be in linkage disequilibrium. Thus, this combination was omitted from the table. Interactions between *TBXA2R* and *ADAM33* and between *IL4RA* and *C3* were suggested for childhood asthma and all asthma. These interactions were our most robust results.

Table 3 Screening of gene–gene interactions

			Effect of SNP 1 on association between SNP 2 and disease[a]			*Association between SNP 2 and disease after stratification by SNP 1*		
SNP 1	*SNP 1 genotype*	*SNP 2*	χ^2	*d.f.*	*P-value*	χ^2	*d.f.*	*P-value*
Childhood asthma								
LTA −735G>A	A/A	*IL12B* 1146C>A	7.12	1	0.0076	18.1	2	0.00012
IL4RA Ile50Val	Ile/Ile	*C3* block2 (haplotype 6)[b]	11.63	1	0.00064	13.42	1	0.00025
TBXA2R 924C>T	C/T	*ADAM33* 313236C>T	9.51	2	0.0086	14.02	2	0.0009
SPINK5 Lys420Glu	G/G	*ADAM33* 313236C>T	12.93	2	0.0016	12.24	2	0.0022
AAA1 522363G>C	C/C	*IL4* 33C>T	10.98	2	0.0041	8.88	2	0.012
AAA1 522363G>C	C/C	*IL4* −590T>C	9.31	2	0.0095	7.67	2	0.022
CCL5 −28C>G	G/G	*IL13* Arg110Gln	7.2	1	0.0073	4.69	1	0.03
CD14 −550C>T	T/T	*IL10* −571C>A	7.1	1	0.0077	4.11	1	0.043
Adult asthma								
SOCS1 −1478CA>del	CA/del	*CTLA4* −318C>T	7.38	1	0.0066	6.36	1	0.012
TNF −1037C>T	T/T	*CCL5* −403A>G	8.51	1	0.0035	5.25	1	0.022
LTA −753G>A	A/A	*SPINK5* Lys420Glu	8.65	1	0.0033	6.95	2	0.031
CD14 −550C>T	T/T	*IL4* −590T>C	11.01	2	0.0041	6.45	2	0.04
All asthma								
TBXA2R 924C>T	C/T	*ADAM33* 313236C>T	12.76	2	0.0017	11.83	2	0.0027
IL4RA Ile50Val	Ile/Ile	*C3* block2 (haplotype 6)[b]	7.29	1	0.0069	6.62	1	0.01
ADAM33 313236C>T	C/T	*TBXA2R* 924C>T	8.05	1	0.0046	8.99	2	0.011
TNF −1037C>T	T/T	*CD14* −159C>T	7.04	1	0.008	7.34	2	0.026
STAT6 GT repeat	172/172	*CC16* 38A>G	11.01	2	0.0041	6.9	2	0.036

Abbreviations: d.f., degree of freedom; SNP, single-nucleotide polymorphism.
[a]Polymorphism combination that demonstrates the interactions with $P<0.01$ and an association with $P<0.05$ are shown.
[b]For haplotype description please refer Inoue *et al.*[11]

DISCUSSION

We conducted our study in three phases. We first, under the assumption of the common disease–common variant hypothesis, investigated whether the 23 most promising asthma/atopy candidate genes retained their association in a Japanese population set. We considered the gene as the unit of our replication, and the gene was judged as positively replicated if demonstrated a statistically significant association with one or more phenotypes (atopic asthma, atopy and total serum IgE level) in at least one of four genetic models. In our samples, among the highly replicated genes (>10 positive associations), *IL13*, *TNF*, *IL4RA* and *ADAM33* maintained their reputation as robust asthma and asthma-related candidate genes. From the genes with a lower replication rate (6–10), we confirmed the associations of *GSTM1*, *GSTP1*, *LTC4S*, *AAA1*, *NOS1*, *CCL5* and *TBXA2R*. In the second phase of the study, we screened our initial significant asthma associations to *IL13*, *TBXA2R*, *GSTP1*, *ADAM33*, *MMP9*, *IL12B*, *C3* and *SOCS1*. These associations were replicated for all genes, except for *TBXA2R* and *GSTP1*, which were associated with atopy and total serum IgE level, respectively. In the final phase, we explored the potential multigenic effect of all 27 candidate genes (the three groups of genes combined) in the expression of asthma phenotypes based on a pairwise method.

If we summarize our findings from the replication study, interesting patterns of associations could be observed. Except for *IL13* and *IL4RA*, we found no association for the prominent genes implicated in innate immunity and immunoregulation with asthma or asthma-related phenotypes, that is, *CD14*, *IL10* and *TGFB1* as well as the Th2 cytokines and their receptors represented by *IL4*, *STAT6* and *MS4A2*. Instead, the genes secreted from airway epithelial cells (for example, *CCL5* and *AAA1*), and genes known to affect lung function, mediate inflammatory conditions and participate in airway remodeling (for example, *TNF*, *ADAM33*, *GSTM1*, *GSTP1*, *LTC4S*, *NOS1* and *TBXA2R*) demonstrated statistically significant associations. This observation may indicate the relatively higher predisposing effect that these two groups of genes exert on the development of asthma-related phenotypes in the Japanese population. Our postulation is supported by the hypothesis that not the dysregulated immune response, but the inherently abnormal respiratory epithelium of asthmatics and the reactivation of the epithelial–mesenchymal trophic unit leading to pathological airway wall remodeling has a major role in the disease.[16,17] Another interesting finding was the distinct partition of genes between adult and child asthma. The association of *LTC4S*, *AAA1* and *CCL5* specifically in the child samples might reflect the differing etiopathogenetic background of childhood asthma.[18,19] For example, *CCL5* is a key chemokine recruiting Th1 and Th2 proinflammatory cells, and its expression in epithelial cells is induced by the respiratory syncytial virus (RSV).[20,21] This is in line with the evidences that the epithelial barrier in young asthmatics is inherently abnormal[22] and that RSV bronchiolitis is a more important risk factor for the development of asthma and atopy up to the age of 7 years than heredity or environmental factors.[23] Moreover, the candidate genes showing significant association with both the phenotypes, when the case groups were compared with adult controls separately (childhood asthma vs adult control and adult asthma vs adult control), were the same as those observed in the combined analysis (all asthma vs all controls). Thus, *TNF*, *ADAM33* and *NOS1* might represent the common susceptibility gene for adult and childhood asthma. When we categorized asthma cases by the age at onset, the number of shared